

Wind Climate Analyses for National Weather Service Stations in the Southeast (U)

Westinghouse Savannah River Company
Savannah River Site
Aiken, SC 29808



This document was prepared in conjunction with work accomplished under Contract No. DE-AC09-96SR18500 with the U. S. Department of Energy.

DISCLAIMER

This report was prepared as an account of work sponsored by an agency of the United States Government. Neither the United States Government nor any agency thereof, nor any of their employees, makes any warranty, express or implied, or assumes any legal liability or responsibility for the accuracy, completeness, or usefulness of any information, apparatus, product or process disclosed, or represents that its use would not infringe privately owned rights. Reference herein to any specific commercial product, process or service by trade name, trademark, manufacturer, or otherwise does not necessarily constitute or imply its endorsement, recommendation, or favoring by the United States Government or any agency thereof. The views and opinions of authors expressed herein do not necessarily state or reflect those of the United States Government or any agency thereof.

This report has been reproduced directly from the best available copy.

**Available for sale to the public, in paper, from: U.S. Department of Commerce, National Technical Information Service, 5285 Port Royal Road, Springfield, VA 22161,
phone: (800) 553-6847,
fax: (703) 605-6900
email: orders@ntis.fedworld.gov
online ordering: <http://www.ntis.gov/help/index.asp>**

**Available electronically at <http://www.osti.gov/bridge>
Available for a processing fee to U.S. Department of Energy and its contractors, in paper, from: U.S. Department of Energy, Office of Scientific and Technical Information, P.O. Box 62, Oak Ridge, TN 37831-0062,
phone: (865)576-8401,
fax: (865)576-5728
email: reports@adonis.osti.gov**

Wind Climate Analyses for National Weather Service Stations in the Southeast

Introduction

Wind speed and direction data have been collected by National Weather Service (NWS) Stations in the U.S. for a number of years and presented in various forms to help depict the climate for different regions. The Savannah River Technology Center (SRTC) is particularly interested in the Southeast since mesoscale models using NWS wind observations are run on a daily basis for emergency response and other operational purposes at the Savannah River Site (SRS).

Historically, wind roses have been a convenient method to depict the predominant wind speeds and directions at measurement sites. Some typical applications of wind rose data are for climate and risk assessment; air pollution exposure and dose calculations; siting industrial plants, wind turbine generators, businesses, and homes; city planning; and air stagnation and high ozone concentration studies.

Common wind rose plots show the conditions on an annual basis for a particular station or group of stations, e.g., Fig. 1. A station's annual wind rose forms a pattern that is often reflective of large-scale weather systems and large or smaller-scale terrain effects such as those in Fig. 1.

Shorter-term wind roses are now being used to present spatial and temporal changes (NCDC, 1995). The NCDC's data has three forms of station frequency tables: annual averages (all hours combined), monthly averages (all hours combined), monthly averages (in standard 3-hr groups, e.g., 01:00, 04:00, 07:00, ... LST). However, these 3-hr frequency tables represent only the wind observations at the listed time, i.e., they are not 3-hr averages.

The purpose of this paper is to demonstrate the overall relationships of wind patterns for NWS stations in the Southeast. Since organized collection of wind data records in the NWS developed rapidly in conjunction with the expansion of commercial aviation after World War II there are now about 50 years of wind speed and direction data available for a large number of NWS stations in this area. In this study we used wind roses for relatively short time scales to show the progression of winds diurnally and monthly to span a typical year. The data used here consist of wind records from 13 National Weather Service Stations in the Southeastern U.S. for approximately 50-year periods. These 13 stations include Augusta (AGS), Athens (AHN), Atlanta (ATL), Columbus (CSG), Macon (MCN) and Savannah (SAV) Georgia; Columbia (CAE) and Charleston (CHS) South Carolina; Asheville (AVL), Charlotte (CLT), Raleigh (RDU), and Wilmington (ILM) North Carolina; and Jacksonville (JAX) Florida. The stations at Savannah (SAV) and Athens (AHN) Georgia had records of 50 and 45 years, respectively. The other stations had 50 or greater years of available data.

Relationships may be discerned for individual stations as a function of diurnal variation and season, as well as among different stations within the region. This is particularly important since these are relatively high quality data from the most recent fifty-year period of record from the NWS.

NWS Wind Instrumentation and Changes in Measurement Height and Location

The equipment used by the NWS for wind speed and direction measurements during the past 50 years has undergone approximately three major changes. First, in the early 1950s the NWS used Aerovane instruments (Middleton and Spilhaus, 1953) to measure winds. From about August 1958 to the mid-1990s the F420 Series wind instruments were used for determining wind speed and direction. Most recently, starting in the mid-1990s wind instruments were switched to the Automated Surface Observing System (ASOS).

The Aerovane instrument was shaped like a “wingless aircraft” with a propeller anemometer at the front to determine wind speed and an aerodynamic tail in the rear to determine wind direction (Middleton and Spilhaus, 1953). The F420 series instruments and the ASOS system have cup anemometer and wind vane separated by about 1 m.

Prior to the automated ASOS system a weather observer used visual/mental averaging to determine the wind speed and direction during a one-minute time period at the top of the hour. The ASOS system uses a two-minute computer average at the top of the hour for both wind speed and direction.

During the period 1950-2000 the NWS wind instruments have undergone not only changes in instrument type but also the location and height of measurement. Table 1 shows the changes that have occurred for the 13 stations of interest in this study.

Table 1. Instrument measurement height ranges, number of changes in location, maximum distance moved, and date of ASOS commission (NCDC).

Station Name	Station Height m (ft) ASL	Wind measurement height (range) after 1950 but prior to ASOS	Number of Location changes after 1950	Maximum horizontal distance moved	ASOS commission date (height change to 10 m)
AGS	40.2 m (131.9 ft)	6.1-7.6 m (20-25 ft)	1	12.1 km (7.5 miles)	05/01/94
AHN	243.8 m (799.7 ft)	6.1-11.0 m (20-36 ft)	2	244 m (800 ft)	02/01/96
ATL	307.8 m (1009.6 ft)	6.1-21.9 m (20-72 ft)	3	1.45 km (0.9 miles)	08/01/95
AVL	652.3 m (2139.5 ft)	9.1 m (20 ft)	1	19.3 km (12 miles)	06/01/96
CAE	64.9 m (212.9 ft)	6.1-11.0 m (20-36 ft)	2	9.3 km (5.8 miles)	12/01/95
CHS	12.2 m (40.0 ft)	9.1 m (20 ft)	1	0.4 km (0.25 miles)	10/01/95
CLT	221.9 m (727.8 ft)	6.1-10.0 m (20-33 ft)	2	503 m (1650 ft)	07/01/98
CSG	119.5 m (392.0 ft)	9.1-9.8 m (32-30 ft)	1	612 m (0.38 miles)	05/01/94
ILM	9.1 m (29.8 ft)	6.1-11.0 m (20-36 ft)	2	6.4 km (4 miles)	11/01/95
JAX	7.9 m (25.9 ft)	6.1-6.4 m (20-21 ft)	2	8.0 km (5 miles)	03/01/96
MCN	107.9 m (353.9 ft)	7.0 m (23 ft)	1	16.1 km (10 miles)	05/01/94
RDU	126.8 m (415.9 ft)	6.1-9.1 m (20-30 ft)	2	16.9 km (10.5 miles)	02/01/96
SAV	14.0 m (45.9 ft)	6.1-9.1 m (20-30 ft)	1	22.9 m (75 ft)	04/01/96

The greatest horizontal displacement in Table 1 is 19.3 km (AVL) and the largest vertical change is 15.8 m (ATL). The remaining stations have typically changed instrument height by about 4 meters prior to reaching the current standard of 10 meters. For the purposes of displaying wind roses it will be assumed that the changes in height and location of a specific NWS station listed in Table 1 are negligible. For other purposes, such as determining changes in the mean speed over the period of record, the changes in sensor height and location will need to be considered.

NWS Wind Speed and Direction Data

Wind speed and direction data for use in this study were obtained for the 13 NWS stations listed above from EarthInfo (EarthInfo, 1996) for time periods beginning in the late 1940s through the mid-1990s. Data were also obtained from the South Carolina Department of Natural Resources (SCDNR) (Brown, 2001) for the balance of the period through the year 2000. (Other possible candidate NWS stations in the Southeast were not included in this study since they did not have a sufficiently long period of wind records.)

Time series plots of the wind speeds at the stations show that “0.0” wind speed or calms were not handled consistently over the entire period for some stations. For particular stations, some time intervals in the data base show no zeros while others contain them, i.e., some periods are missing the calm wind observations. Missing calm winds are not particularly relevant to the wind rose plots presented in this report since they have no associated direction, and no attempt was made to correct any data obtained from EarthInfo and the SCDNR.

Table 2 shows the total years of data and the percentage of the total number of observations with missing and calm wind directions and speeds. Both AGS (in late 1980s) and CSG (during 1950s to mid-1960s) had periods when no observations were made during nighttime hours, especially the six hours after midnight. The percentage of missing wind directions at CSG is the highest at 40%, but the percentage missing at AGS is not significantly different than the other stations. However, during the discussions in the following sections it may be useful to be aware that AGS and CSG have a disproportionate number of missing wind directions during the pre-dawn hours, and CSG has a fairly large percentage of missing data.

Table 2. Percentage of the total number of observations with missing wind directions for the 13 Southeast stations used in this study for periods beginning in the late 1940s and early 1950s through December 31, 2000.

Station Name	Percent of missing and calm wind directions	Percent of missing and calm wind speeds	Total Years of data
AGS	27.7	13.6	52
AHN	30.1	24.6	45
ATL	6.1	0.7	52
AVL	31.5	10.3	52
CAE	24.3	10.3	52
CHS	17.2	10.3	52
CLT	19.3	10.3	52
CSG	40.4	29.5	51
ILM	28.4	19.1	52
JAX	16.0	5.1	52
MCN	26.2	14.9	52
RDU	18.2	7.7	52
SAV	26.2	17.4	50

In order to show the data for all years on a wind rose plot, it is necessary to convert the wind directions during the period 1964-2000 into 16-point compass sector wind directions, since those winds were reported to the nearest 10 degrees. This was accomplished by adding a random number between -5 and +5 to the reported wind direction and then converting the wind direction to the nearest compass point (N, NNE, etc.) This removes a bias for certain compass points near the 10-degree-rounded wind directions.

With the quantity of data available it was possible to average the data for the wind rose plots in different ways to examine the climatic changes over a typical year. Data were first categorized and averaged by season (winter; December, January, and February; spring; March, April, and May; summer; June, July, and August; autumn; September, October, and November) and periods of a day. The set of four periods: pre-rise – 00:00-05:00 LST; morning – 06:00-11:00 LST; afternoon – 12:00-17:00; evening – 18:00-23:00 LST; with 6 hourly observations in each period span a typical day. For more detailed analysis we decided to focus on twenty-six two-week periods spanning a typical year and six 4-hr time periods covering the diurnal cycle. The six 4-hr time periods selected were (midnight, 00:00-03:00 LST; pre-rise, 04:00-07:00; post-rise, 08:00-11:00; afternoon,

12:00-15:00; early evening, 16:00-19:00; late evening, 20:00-23:00 LST). For a single station in each wind rose plot during the time period January 1, 1951 to December 31, 2000 (50 years) there are 438,312 total hourly observations. Using the four-seasons, four-times of day averaging scheme this amounts to 27,394 hourly observations that are represented for a single station in an individual wind rose plot. For the 26 2-week periods covering the year and six 4-hr periods spanning a day, there are about 2810 hours of data at a single station represented in each individual wind rose plot.

For the latter case, a complete set of 156 (26 x 6) wind roses are available on the Internet at an address provided by the author (allen.weber@srs.gov). This method of presenting the wind rose plots was chosen as a practical matter since there were too many color figures to be reasonably accommodated in printed form. In this printed report we will present and describe the figures representing the four annual seasons and the four periods of the day. We will also show a few examples illustrating the diurnal cycle with a few special cases of interest.

Geographical Features and Observed Annual and Seasonal Changes in Wind Direction

The Southeast's major terrain features are the Appalachian Mountains and the Atlantic Ocean. The mountains are oriented from the southwest to the northeast as is the coastline. The mountains give way to smoother terrain in north Georgia but their slope is generally from the southwest to the northeast with local variations superimposed. Fig. 1 shows that the station at Asheville, North Carolina (AVL) is totally dominated by the influence of the north-northwest -- south-southeast oriented French Broad River valley that cuts through the mountains. The river drainage near Asheville is basically from the SSE to the NNW. AVL's terrain influence is so strong on the wind directions that variations in its wind rose will be mostly omitted from the seasonal and diurnal discussions below. The coastal plains and the Atlantic Ocean beyond the seacoast provide a temperature gradient favorable for the production of sea/land breezes, particularly in the spring and summer.

The annual wind rose patterns (Fig. 1) at AGS, SAV, JAX have a certain degree of isotropy, but both the annual and spring patterns (Fig. 2) show that ATL, AHN, MCN, CLT, CAE and RDU are influenced by the high terrain presented by the Appalachian Mountains. It can be seen in these same two figures that northwesterly and westerly winds occur more frequently at ATL, CSG, MCN, AHN, and to some extent even AGS. These stations show the steering effects on cyclonic systems passing the Appalachians from the west or southwest. The higher terrain of the Appalachians also influences the wind measurements at CAE, CLT, and RDU and, given their location on the lee side of the mountains, show more frequent southwesterly winds. In springtime the patterns of the coastal stations show more pronounced onshore flow, as sea breezes become more common.

In the summer (Fig. 3) the sea breezes show slightly increased frequency for the coastal stations but the wind roses obscure some of the sea breeze effects because of land breezes

and the Bermuda high pressure system that helps produce along-shore flow in the summer (discussed later). The inland stations show strong influence from the Appalachian Mountains except AGS, which has a lobe of stronger winds from the southeast due to channeling of the winds along the Savannah River corridor and sea breeze penetration inland from the coast.

In autumn (Fig. 4) all stations show increased frequencies of wind out of the northeast, a consequence of the high-pressure systems that are frequently centered over the Eastern U. S. This effect was also noted several years ago using ship observations in the South Atlantic Bight (Weber and Blanton, 1980).

In winter (Fig. 5) the northeasterly winds give way to predominately northwesterly or westerly winds arising from the storm track of approaching cyclonic systems at CSG, ATL, MCN, AHN, and AGS (all Georgia stations). All stations in both South Carolina and North Carolina show winds predominately from the southwest or from the northerly sectors as cyclonic systems are either forced around or track south of the southern tip of the Appalachians. There is also cold air damming in the lee of the Appalachians when high-pressure systems to the north or east pile air against the eastern slope of the Appalachians.

Observed Seasonal and Diurnal Changes in Wind Direction

Figures 6-9 show the diurnal breakdown for the spring season. All the coastal stations show a significant increase in southwesterlies for the pre-sunrise hours that is not as apparent in the overall spring pattern. CLT and RDU become more southwesterly in the morning hours than in the pre-sunrise hours. Spring afternoons and evenings (Fig. 8 and 9) show significant increases in sea breeze occurrences. Indeed, the sea breeze is strongly evident as far inland as AGS (\approx 200-km inland, as seen in simulations by Buckley and Kurzeja, 1997, and described by Kurzeja, Berman, and Weber, 1991).

The summer pre-sunrise pattern (Fig. 10) is quite different from the corresponding spring pattern (Fig. 6). Wind directions for the coastal stations have shifted to more along-shore flow for the coastal stations. There are strong indications that channeling along the Savannah River continues to influence AGS. Southwesterly flow is frequent for CAE and RDU during these pre-sunrise hours. However, CSG has more frequent northeasterly wind directions. This may be due to local high terrain to the north of CSG. During summer mornings (Fig. 11) the coastal stations seem to have their wind direction shifted clockwise so as to become more west-southwesterly. The inland stations show a similarity to the pre-sunrise patterns except for AGS, which has lost most of the vestiges of the sea breeze and channeling lobes from the south through southeast. The summer afternoon pattern (Fig. 12) shows a significant channeling influence, whereas other inland stations (CAE AND MCN) are more isotropic in their appearance. The summer evening pattern (Fig. 13) shows strong preferential onshore flow from channeling and sea breezes that reach inland as far as AGS and RDU, both of which have their largest on-shore wind lobe for any season and time of day.

The autumn pre-sunrise (Fig. 14) wind roses show the dramatic change in wind direction that accompanies the change to cooler temperatures. The wind has shifted from predominately southwesterly along the coast to predominately northeasterly. CAE and RDU are about equally divided between southwesterly and northeasterly flow while ATL, AHN, and CSG show strong lobes from the northwest and northeast. Only AGS seems to be uninfluenced by the northeasterly flow because of the preferential drainage and channeling of winds along the Savannah River basin. This pattern is repeated for autumn mornings (Fig. 15) however, by afternoon (Fig. 16) most of the stations except for JAX, ATL, AHN, MCN, and CAE show more isotropic patterns for the wind directions.

All four of the diurnal patterns for winter (Figs. 18-21) have shifted from northeasterly flow and are basically similar to the overall winter wind roses (Fig. 5). Winter evenings (Fig. 21) show increased along-shore and onshore components of the wind. Winter evenings' wind rose patterns closely resemble those for pre-sunrise (Fig. 18).

Discussion of Wind Roses

- Diurnal changes

Diurnal changes linked to the sea breeze phenomena can be seen for all the coastal stations. Sea breezes are expected to be nearly perpendicular to the coast but seem to veer as time progresses into evening and pre-sunrise hours. Climatologically, loss of the atmospheric frictional force after sundown causes the wind to begin an inertial oscillation with a period of $2\pi/f$ where f is the Coriolis parameter. An inertial oscillation within the latitude range of these Southeast stations (around 31-34 degrees north) would be on the order of 21-23 hrs and might typically begin after 17:00 LST, shifting about 16-17 degrees per hour during the evening hours. However, a complete inertial oscillation requires a wind shift of about 90 degrees in 6 hours of time, whereas these data show only about a 45-degree shift between the figure for summer evening (Fig. 13) and summer pre-sunrise (Fig. 10). The complete clockwise rotation of the predominant wind in these wind roses may be obscured by the time averaging (6-hrs) of the wind data coupled with the fact that the frictional force is not totally absent in these near surface measurements. Another possible explanation for the incomplete wind rose mode rotation is the influence of the subtropical high-pressure system, which is a dominant factor in the North Atlantic in the summer. The mean position of the subtropical high tends to produce an along-shore component of the wind in summer.

- Sea breeze penetration to AGS, CAE, and RDU

The channeling effect of the Savannah River basin and the sea breeze influence on AGS are apparent in the strong southeast lobes in the spring, summer, and autumn evenings (Figs. 9, 13, and 17) and even to some extent in the spring and summer afternoons (Figs. 8 & 12). Considering the distance to the nearest coastline there are even hints that RDU,

CLT, and CAE receive sea breezes in the spring and summer evenings since those stations have preferential lobes from the south.

- Drainage flow

A drainage flow is expected down the Savannah River along the border separating South Carolina and Georgia and is evident in the autumn pre-sunrise and morning wind roses in Figs. 14 and 15. This drainage flow seems to predominate over the northeasterly flow found at the remaining stations. The drainage flow might also be expected near CSG since it lies near a river as well. The higher resolution data (two-week – 4-hour averages) do show a secondary maximum from the north-northwest along the Chattahoochee River, however one must also recall that CSG had a large number of missing early morning observations during the 1950s to mid 1960s.

- Orographic effects -- Influence of the Appalachians

The Appalachian Mountains have a pronounced effect on the surface wind flow for all seasons. The effect is best seen in the afternoon hours in Figs. 8, 12, 16, & 20 where the wind roses for stations at ATL and AHN show the effect the mountains have on storm systems approaching from the west or southwest and passing through to the northeast. Also, it can be seen that ATL's winter pre-sunrise wind rose in Fig. 18 has winds predominately from the northwest, whereas AHN's predominate lobe is west-northwest.

- Similar groups

The wind roses discussed so far seem to suggest groupings of similar stations, e.g., the stations nearest the Appalachians; ATL and AHN, and MCN. The second major group is the coastal stations ILM, CHS, SAV, and JAX. The wind roses for the piedmont stations of CLT, RDU and CAE seem to resemble each other closely much of the time. The wind directions for CLT are somewhat ambiguous, since it is closer to the mountains than the other two stations in this group. AGS, like AVL, seems to be in a group by itself.

Wind speeds

The wind speed time series were examined for the period that data was supplied for each station. Careful visual inspection of time series plots (not shown here) showed suspicious changes or breaks in the record most likely due to changes in instrumentation, method of making the observation, or both. It was also apparent that the calms were handled differently during some periods. Also, the National Weather Service (Brown, 2001) took observations every three hours in the late 1960s to early 1970s as an economy measure. These features of the time series are shown in Table 3 along with some remarks about differences in the distribution function among the time series breaks. It appears that ATL is the only station that has a completely homogeneous time series for the 50-year period.

Table 3. Characteristics of NWS station 50-year time series plots and distributions of wind speeds. Numbers in the table refer to the year, e.g., 65 = 1965.

NWS Station	Time series breaks (determined by examining plots of the wind speed time series over the period of record)	CHD – period (visual inspection of the time series showed that calms were handled differently)	3-hour interval reporting	Remarks on distributions (DSD – distribution significantly different due to calms)
AGS	50-65 65-74 74-00	CHD – 49-50	65-74	DSD 75-00
AHN	48-65 65-82 82-00	CHD – 96-00	65-82	Shapes similar
ATL	NONE			
AVL	48-65 65-73 73-00	CHD – 48-64	65-73	DSD 48-65
CAE	48-65 65-73 73-00	CHD – 96-00	65-73	DSD 48-65
CHS	48-65 65-70 70-75 75-78 78-00	Fairly uniform	65-70 75-78	Uniform shape
CLT	48-65 65-73 73-00	CHD – 53-61	65-73	DSD 48-65
CSG	48-65 65-81 81-00	CHD – 54-62	65-81	DSD 48-64
ILM	48-65 65-78 78-00	CHD – 56-60	65-78	DSD 48-65
JAX	48-66 66-70 70-00	CHD – 52-70	66-70	DSD 70-00
MCN	49-65 65-74 74-00	Fairly uniform	65-74	Uniform shape
RDU	49-65 65-72 72-00	CHD – 96-00	65-72	Small differences in low speeds and calms
SAV	51-65 65-78 78-00	CHD – 51-78	65-78	Differences in 1 st two periods in calms

In view of these differences among the breaks in the time series identified in Table 3 it was decided to use the period of each station’s record between 1966 and 1993 inclusive

for investigating the wind speed variations. This 28-year period includes the most completely homogeneous data set that could be extracted from the data provided for each station so that spectral analysis could be performed.

A plot showing the wind speed averaged for each hour of the day is shown in Fig. 22 for the period from 1966-1993. This figure shows the average diurnal variation of winds near the surface for the Southeast stations. All stations show the minimum speed at night between 03:00-06:00 LST, and the maximum in the afternoon between 13:00 and 16:00 LST in every case except RDU and AGS. The RDU plot shows some small secondary maxima that not present in the other stations, while AGS's minimum wind speed occurs around midnight. It is of interest to note that ATL's nighttime minimum wind speed is considerably higher than the other stations in the Southeast while its daytime maximum wind speed is lower than five of the other stations. The reason for this might be due to the tower's siting in the large metropolitan Atlanta area.

The wind speed averaged for all stations by month is shown as a time series in Fig. 23 for the period from 1966-1993. This figure shows little change in the characteristics of the wind speed during the 28-year period. Fig. 23 shows the annual cycle with a minimum and maximum each year. Some years show a decreased range (lower maximum and higher minimum than other years (for example 1976-77). There appears to be more of these shorter wind-speed-range periods in the latter part of the time series than in the earlier part. Another interesting feature is that the time series often show a secondary maximum and minimum within a given yearly cycle, i.e., as speed-up followed by a drop-back in speed. These changes in wind speed are not always particularly significant in terms of the actual magnitude of the change, however.

The mean monthly time series for all stations is shown in Figs. 24-27. Figure 24 shows that JAX has the lowest wind speeds for the coastal stations and CHS is generally the highest. Figure 25 shows that RDU is generally the highest for the Piedmont stations while CAE is the lowest. Figure 26 shows that ATL is highest for the Southern Appalachian stations while CSG is generally the lowest. Figure 27 shows the two remaining stations, AGS and AVL (which do not fit logically in the other groupings).

The time series can be averaged for each station by month and the results are presented in Fig. 28. This figure shows again that AGS has the lowest and ATL the highest wind speed. The highest wind speeds during a typical year are achieved in March while the lowest is in August (except for AGS which is lowest during September by a small amount). CHS has the second highest wind speeds and ILM the third.

The annually averaged wind speed for each station is show as a time series in Fig. 29. There is a biennial oscillation evident that is in phase across the majority of the stations. Occasionally one or two stations get out of phase with the others, e.g., SAV and CAE in 1980. Careful observation also indicates the presence of a longer period oscillation as well. The ensemble average for all stations is shown in Fig. 30. Fig. 31 shows the spectral density of the ensemble of the monthly-averaged wind speeds. This figure shows a "split

biennial” oscillation as well as periods of 3.4 years and about 10 years. The “split biennial” period refers to the two peaks on either side of 2 years. These peaks are so close together that they might be manifestations of the same biennial peak. On the other hand, they may be indications of two different underlying physical phenomena.

Individual station power spectra are shown in Figs. 32-44. The power spectral density for AVL seems to depict the known period of El Nino best. The origin of the biennial oscillation in the time series might be linked to the biennial oscillation in the equatorial stratosphere. More research will be needed to clarify these relationships.

Conclusions and Recommendations

Wind speed and direction information has been collected by the NWS for many years at several stations in the Southeast but not a great deal has been done to summarize and present these data in readily understandable forms. This report has been written to help rectify this and to point out some features of the wind speed and direction that have not been widely recognized in the past. Short-term (two-week) wind roses available on the Internet provide a means to demonstrate the temporal and spatial relationships that wind speed and direction undergo using a fifty-year database from 13 stations in the Southeast.

In order to present the wind roses in this report in a consistent manner the NWS observations made from 1964 to present (normally rounded to the nearest 10 degrees of azimuth) were processed by adding a random number between -5 and +5 to the reported wind direction. Those directions were then converted to the nearest compass point (N, NNE, etc.) This removes a bias for certain compass points near the 10-degree-rounded wind directions that would otherwise occur if one uses an ordinary rounding scheme. Wind data were broken down into monthly, seasonal, biweekly and six periods of the day from a total of around 438,312 hourly observations in order to bring out the relationships.

The Appalachian Mountains and the Atlantic Ocean proved to be major influences of wind direction for this group of Southeast stations. Terrain steering of the wind is suggested in the seasonal and diurnal patterns of the wind. In addition AGS is strongly influenced by channeling and sea breezes that penetrate up the Savannah River in the spring and summer seasons. Sea breeze influence can also be seen for RDU, CLT, and CAE as well. In autumn all stations are subject to a strong northeasterly wind that arises from high-pressure systems to the north and northeast. Sea and land breezes are evident along the Southeast Coastal stations. An inertial oscillation of the wind seems to be evident in the wind roses for these stations as well.

Separate time series plots of the wind speed for several stations (not included in this report) show suspicious changes or breaks in the record most likely due to changes in instrumentation, method of making the observation, or both. It appears that ATL is the only station that has a completely homogeneous time series for the 50-year period. Among the 13 stations AGS has the lowest wind speeds and ATL has the highest. Also, JAX has the lowest wind speeds for the coastal stations whereas CHS is generally the

highest. The highest wind speed for a typical year is in March while the lowest is in August. If one averages all 13 stations to get an ensemble average by month there is a biennial oscillation in the wind speed. There are peaks in the power spectrum of the wind speed at 3.4 and 10 years. More research is needed to identify the cause of these periodic components.

Acknowledgements

The authors would like to acknowledge the assistance of M. E. Brown, Acting State Climatologist for the state of South Carolina, who provided the NWS Southeast stations' data. The authors would like to acknowledge the able assistance of L. D. Koffman for his help with the wind rose plots using ArcView GIS.

References

- Brown, M., 2001: Meteorological Data for Several Stations in the Southeast. South Carolina Department of Natural Resources, Columbia, SC (USA).
- Buckley, R. L., and R. J. Kurzeja, 1997: An observational and numerical study of the nocturnal sea breeze. Part I: structure and circulation. *J. Appl. Meteor.*, **36**, 1577-1598.
- EarthInfo, Inc., 1996: NCDC Surface Airways, Boulder, CO (USA).
- R. J. Kurzeja, S. Berman, A. H. Weber, 1991: A climatological study of the nocturnal planetary boundary layer., *Bound.-Layer Meteor.*, **36**, 105-128.
- Middleton, W. E. K. and A. F. Spilhaus, 1953: Meteorological Instruments, 3rd ed., University of Toronto Press, Toronto, Canada.
- NCDC: Station Location. NCDC Subscription Services Center, 310 State Route 956, Building 300, Rocket Center, WV 26726.
- NCDC and USAFETAC OL-A, 1995: International Station Meteorological Climate Summary, Ver. 3.0, March 1995.
- Weber, A. H. and J. O. Blanton, 1980: Monthly mean wind fields for the South Atlantic Bight, *Journal of Physical Oceanography*, **10**, 1256-1263.

List of Figures

Fig. 1. Map showing the 13 Southeast NWS station windroses used in this study for all seasons and all periods of the day. The “petal” lengths are all normalized to the 20% segment shown. The six wind speed classes are 0-2, 2-4, 4-6, 6-8, 8-12, and < 12 m/s. The elevation contours, beginning at 50 m, are shaded every 50 m.

Fig. 2. As in Fig. 1 except for the spring season (March, April, & May).

Fig. 3. As in Fig. 1 except for the summer season (June, July, and August).

Fig. 4. As in Fig. 1 except for the autumn season (September, October, & November).

Fig. 5. As in Fig. 1 except for the winter season (December, January, and February).

Fig. 6. As in Fig. 1 except for the spring season and the pre-sunrise hours of day (00:00 – 05:00 LST).

Fig. 7. As in Fig. 1 except for the spring season and the morning hours of day (06:00 – 11:00 LST).

Fig. 8. As in Fig. 1 except for the spring season and the afternoon hours of day (12:00 – 17:00 LST).

Fig. 9. As in Fig. 1 except for the spring season and the evening hours of day (18:00 – 23:00 LST).

Fig. 10. As in Fig. 1 except for the summer season and the pre-sunrise hours of day (00:00 – 05:00 LST).

Fig. 11. As in Fig. 1 except for the summer season and the morning hours of day (06:00 – 11:00 LST).

Fig. 12. As in Fig. 1 except for the summer season and the afternoon hours of day (12:00 – 17:00 LST).

Fig. 13. As in Fig. 1 except for the summer season and the evening hours of day (18:00 – 23:00 LST).

Fig. 14. As in Fig. 1 except for the autumn season and the pre-sunrise hours of day (00:00 – 05:00 LST).

Fig. 15. As in Fig. 1 except for the autumn season and the morning hours of day (06:00 – 11:00 LST).

Fig. 16. As in Fig. 1 except for the autumn season and the afternoon hours of day (12:00 – 17:00 LST).

Fig. 17. As in Fig. 1 except for the autumn season and the evening hours of day (18:00 – 23:00 LST).

Fig. 18. As in Fig. 1 except for the winter season and the pre-sunrise hours of day (00:00 – 05:00 LST).

Fig. 19. As in Fig. 1 except for the winter season and the morning hours of day (06:00 – 11:00 LST).

Fig. 20. As in Fig. 1 except for the winter season and the afternoon hours of day (12:00 – 17:00 LST).

Fig. 21. As in Fig. 1 except for the winter season and the evening hours of day (18:00 – 23:00 LST).

Fig. 22. A typical diurnal cycle for each station. Wind speeds averaged for each hour of the day (00:00-23:00) for all thirteen NWS stations.

Fig. 23. Time series of the ensemble (all stations averaged) of monthly-averaged wind speeds from 1966-1993.

Fig. 24. As in Fig. 22 except for coastal stations (CHS, ILM, JAX, and SAV).

Fig. 25. As in Fig. 22 except for piedmont stations (CAE, CLT, and RDU).

Fig. 26. As in Fig. 22 except for southern Appalachian stations (AHN, ATL, CSG, and MCN).

Fig. 27. As in Fig. 22 except for remaining stations (AGS and AVL).

Fig. 28. Monthly averaged wind speeds for all 13 stations plotted by month (January-December).

Fig. 29. Annually averaged wind speeds for all 13 stations plotted by year (1966-1993).

Fig. 30. Time series of the ensemble (all stations averaged) of annually-averaged wind speeds (1966-1993).

Fig. 31. Power spectral density of the time series in Fig. 22 (truncated prior to the dominant annual cycle).

Fig. 32. Power spectral density of the monthly-averaged wind speed time series for AGS (truncated prior to the dominant annual cycle).

Fig. 33. Power spectral density of the monthly-averaged wind speed time series for AHN (truncated prior to the dominant annual cycle).

Fig. 34. Power spectral density of the monthly-averaged wind speed time series for ATL (truncated prior to the dominant annual cycle).

Fig. 35. Power spectral density of the monthly-averaged wind speed time series for AVL (truncated prior to the dominant annual cycle).

Fig. 36. Power spectral density of the monthly-averaged wind speed time series for CAE (truncated prior to the dominant annual cycle).

Fig. 37. Power spectral density of the monthly-averaged wind speed time series for CLT (truncated prior to the dominant annual cycle).

Fig. 38. Power spectral density of the monthly-averaged wind speed time series for CSG (truncated prior to the dominant annual cycle).

Fig. 39. Power spectral density of the monthly-averaged wind speed time series for CHS (truncated prior to the dominant annual cycle).

Fig. 40. Power spectral density of the monthly-averaged wind speed time series for ILM (truncated prior to the dominant annual cycle).

Fig. 41. Power spectral density of the monthly-averaged wind speed time series for JAX (truncated prior to the dominant annual cycle).

Fig. 42. Power spectral density of the monthly-averaged wind speed time series for MCN (truncated prior to the dominant annual cycle).

Fig. 43. Power spectral density of the monthly-averaged wind speed time series for RDU (truncated prior to the dominant annual cycle).

Fig. 44. Power spectral density of the monthly-averaged wind speed time series for SAV (truncated prior to the dominant annual cycle).

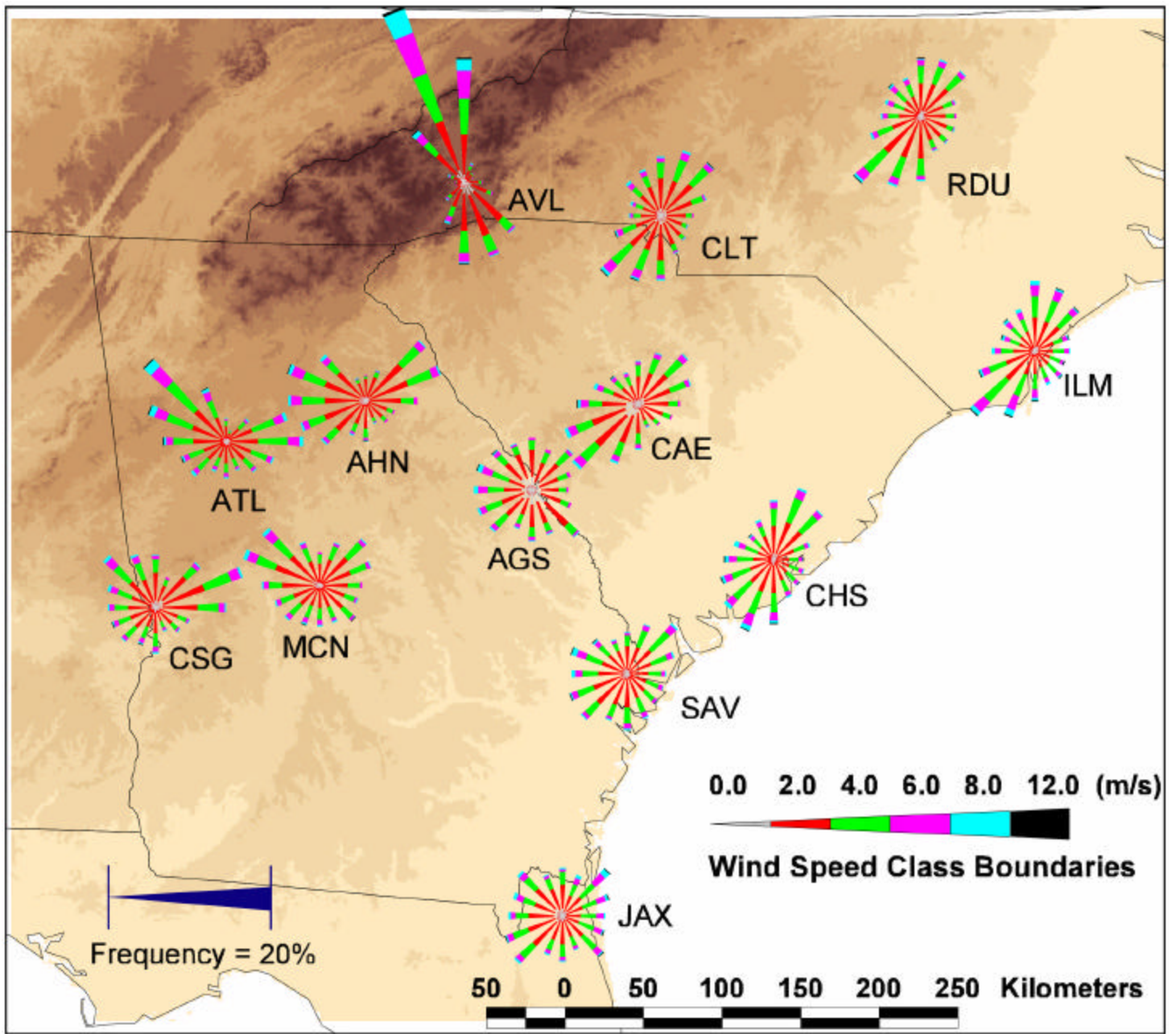


Figure 1: Annual wind roses for various NWS sites in the Southeastern U.S.

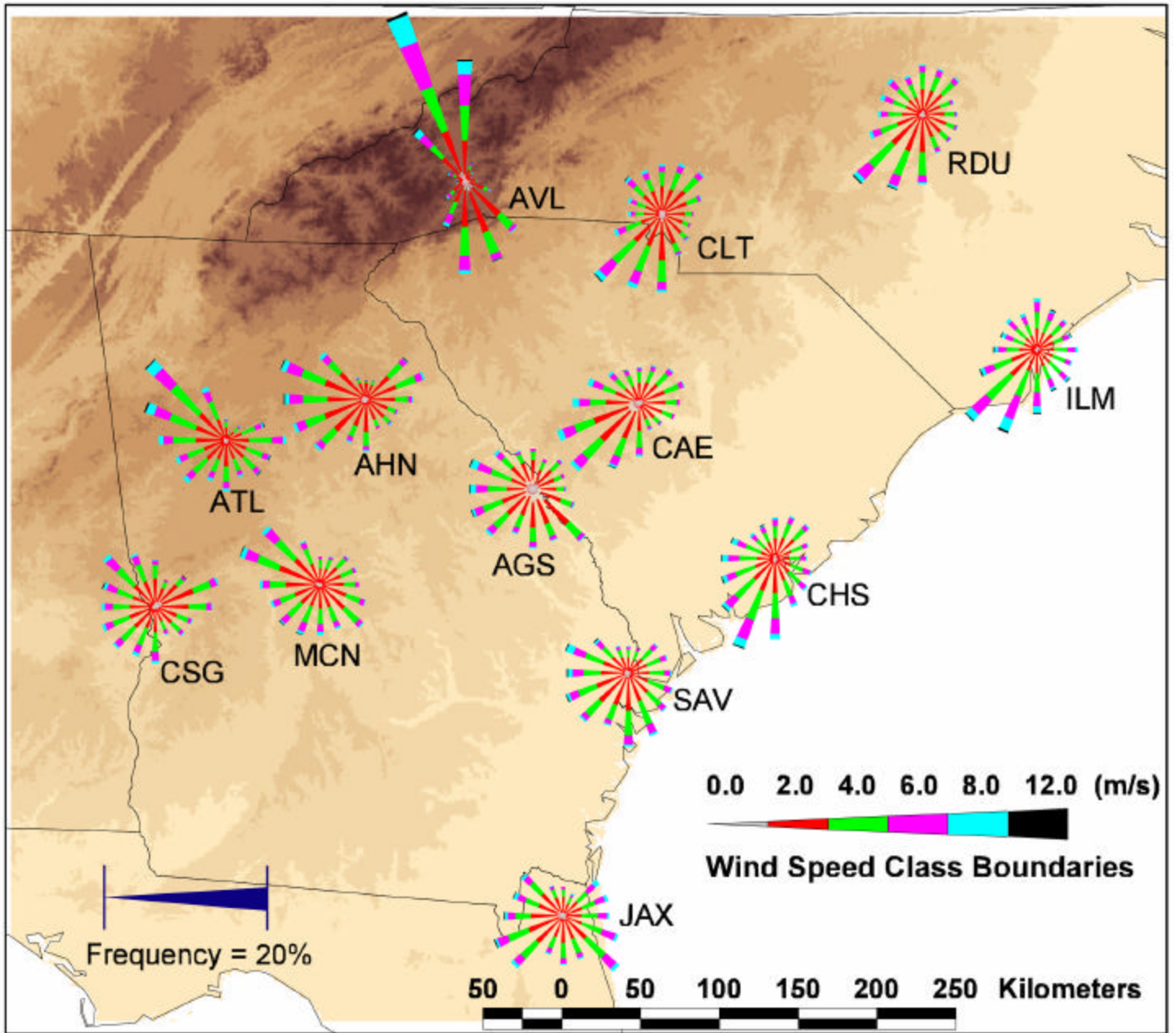


Figure 2. Spring (March, April, May)

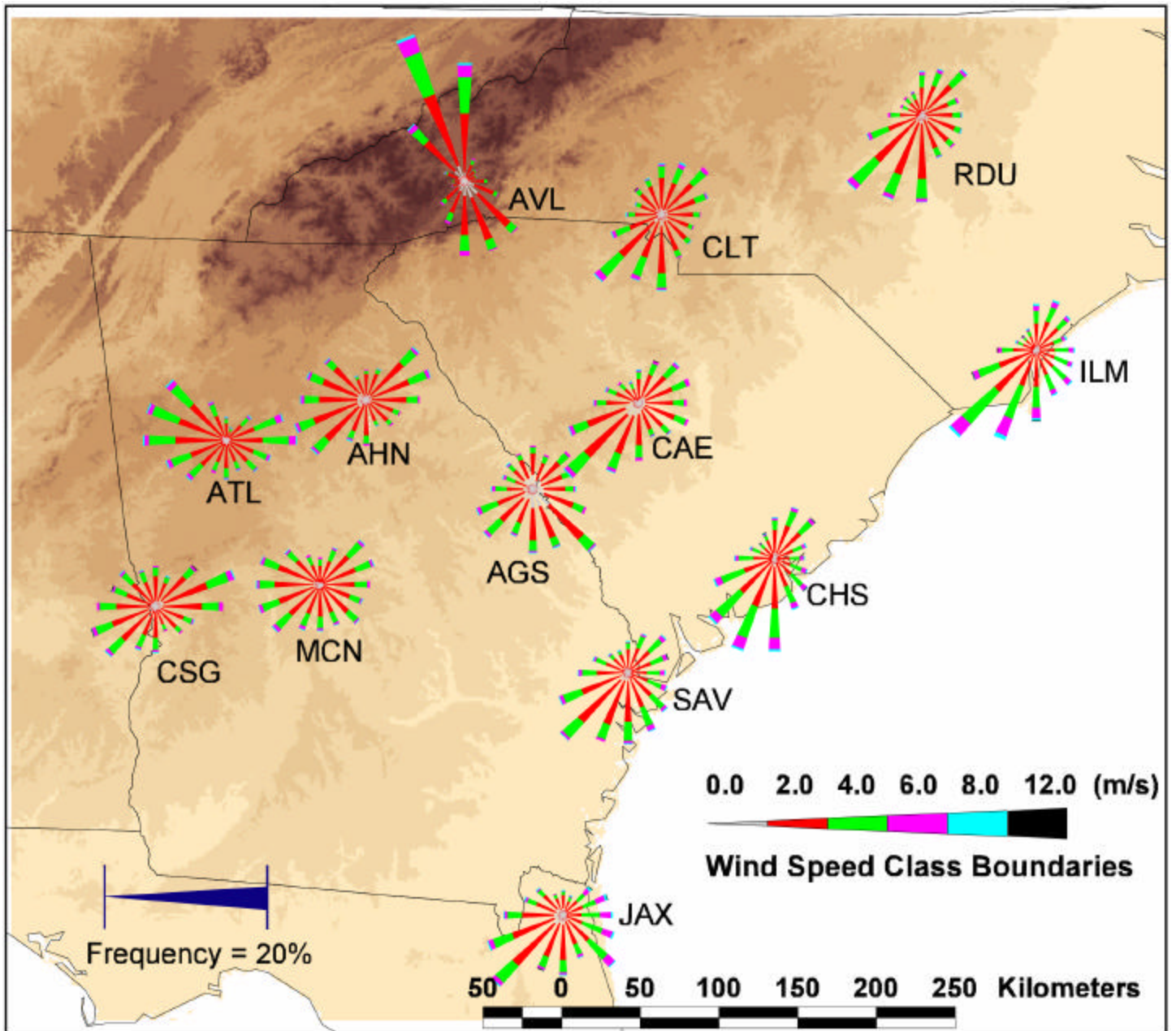


Figure 3. Summer (June, July, August)

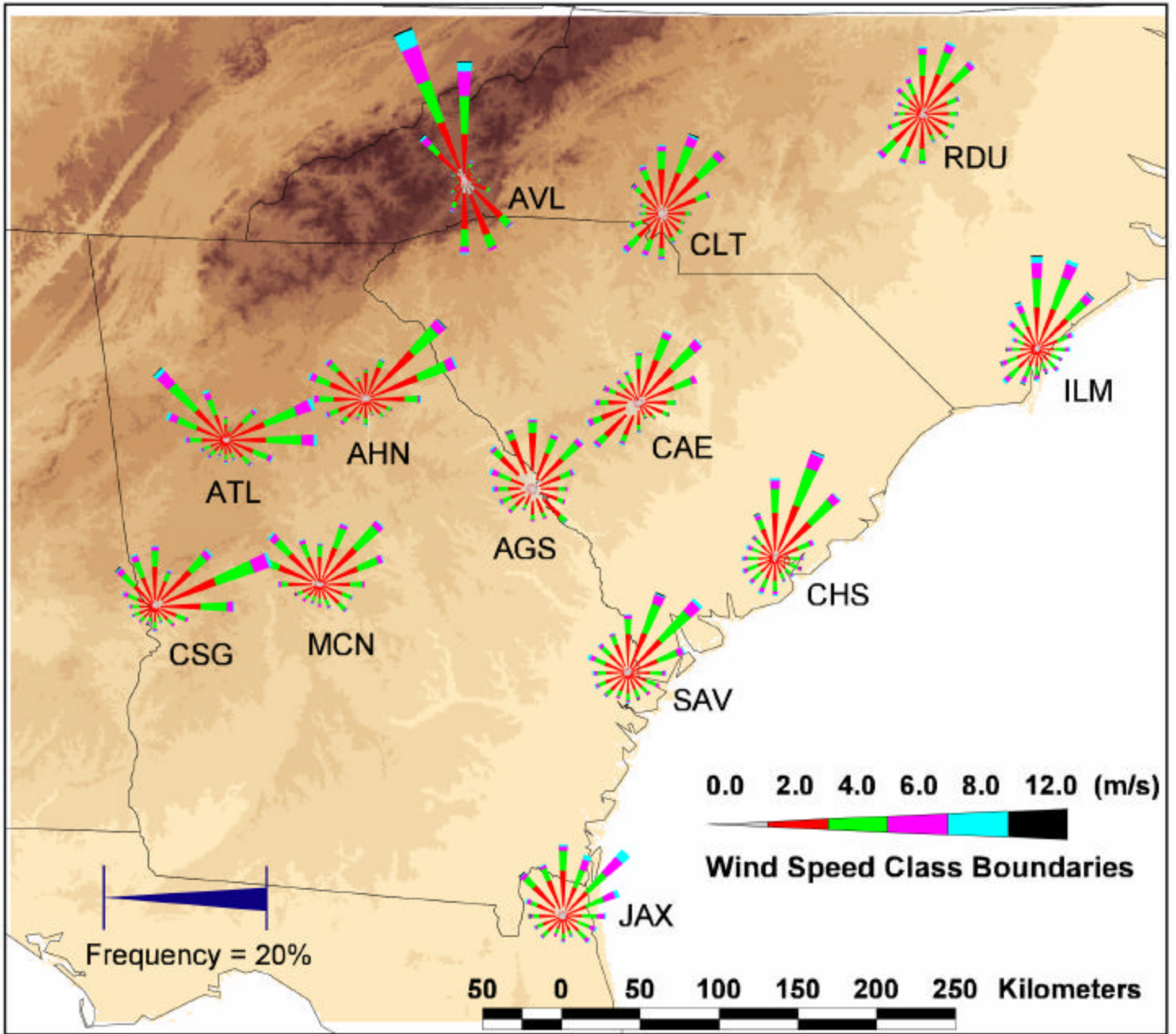


Figure 4. Autumn (September, October, November)

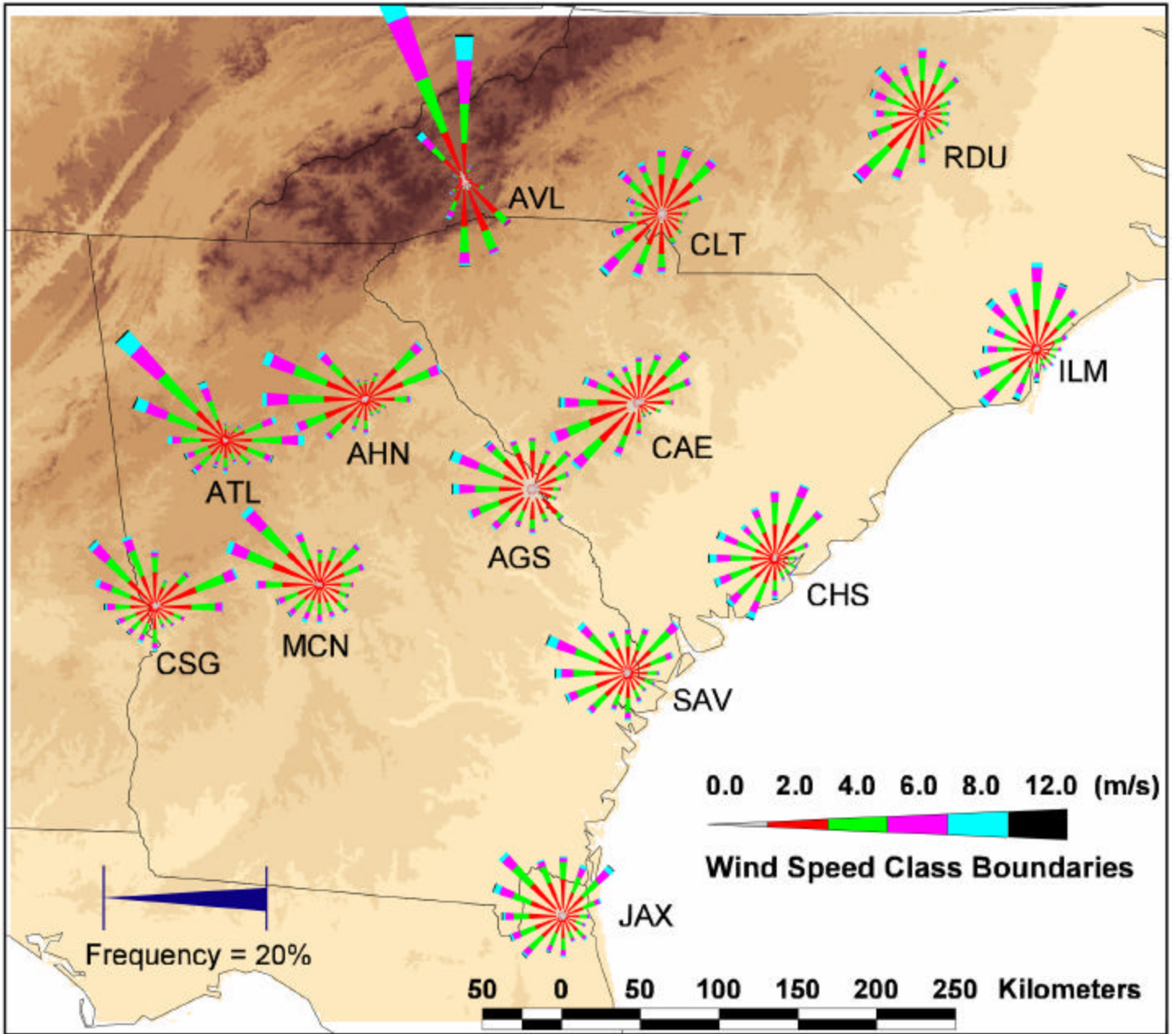


Figure 5. Winter (December, January, February)

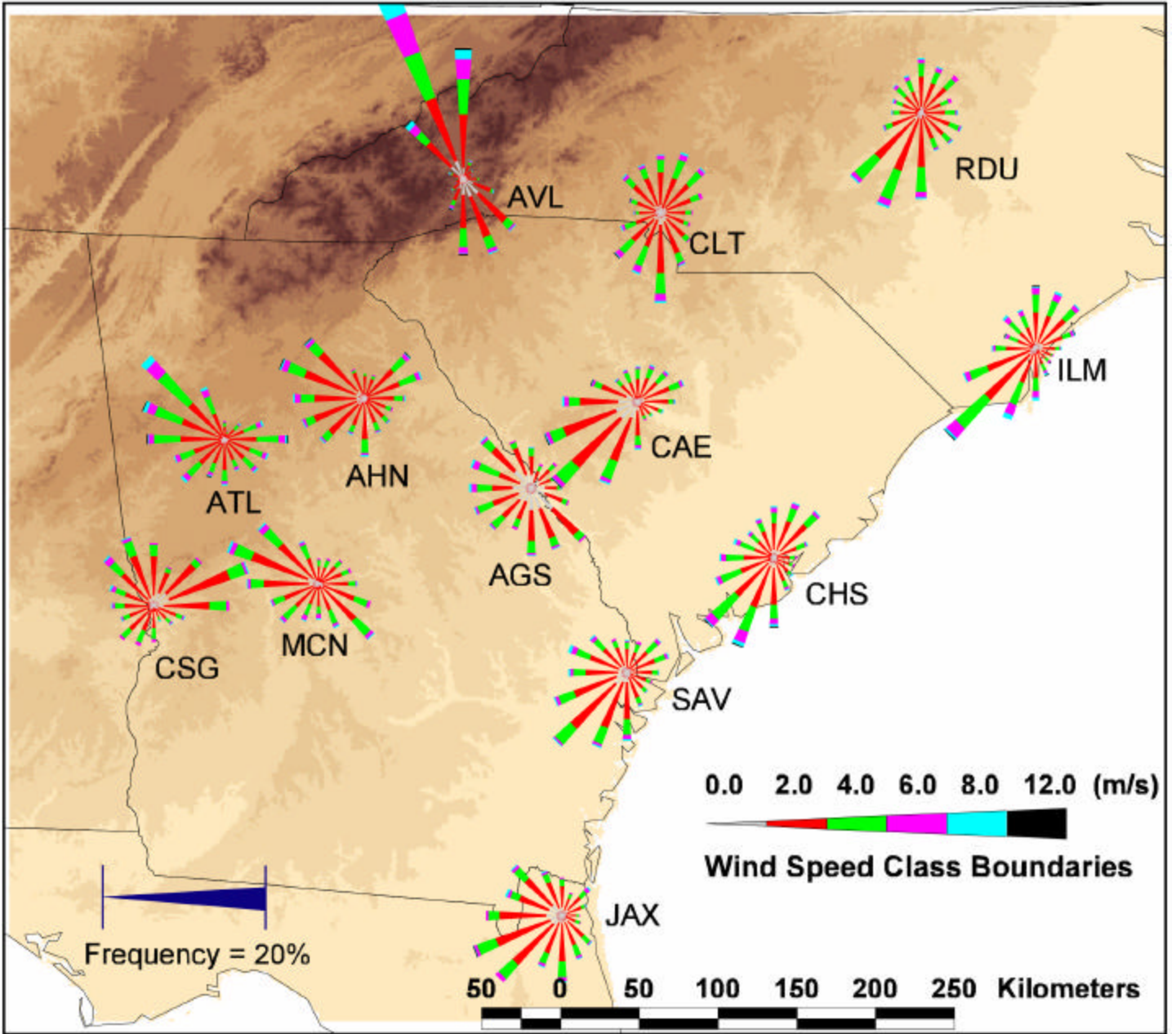


Figure 6. Spring pre-sunrise (00:00-05:00 LST).

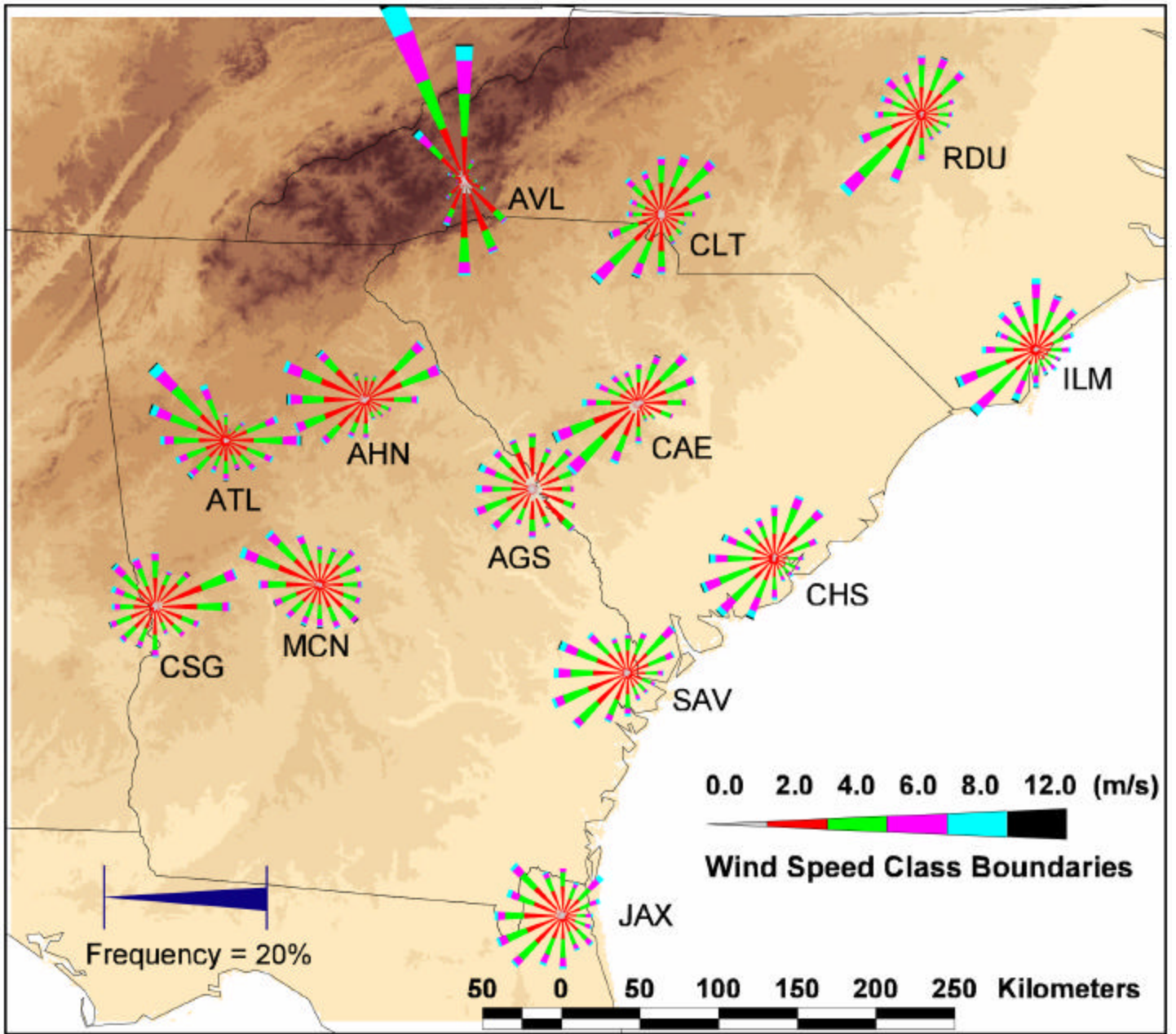


Figure 7. Spring morning (00:06-11:00 LST).

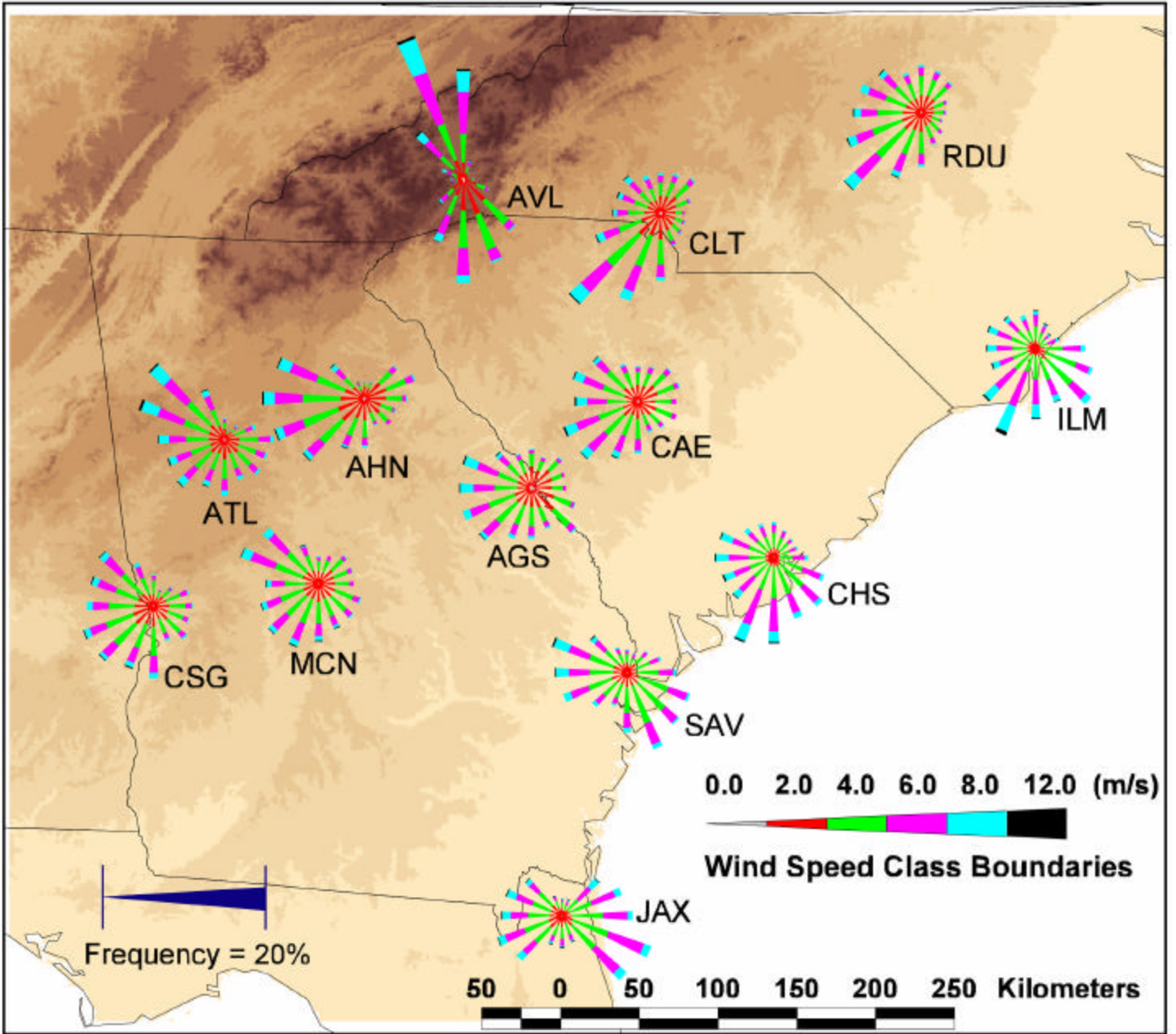


Figure 8. Spring afternoon (12:00-17:00 LST).

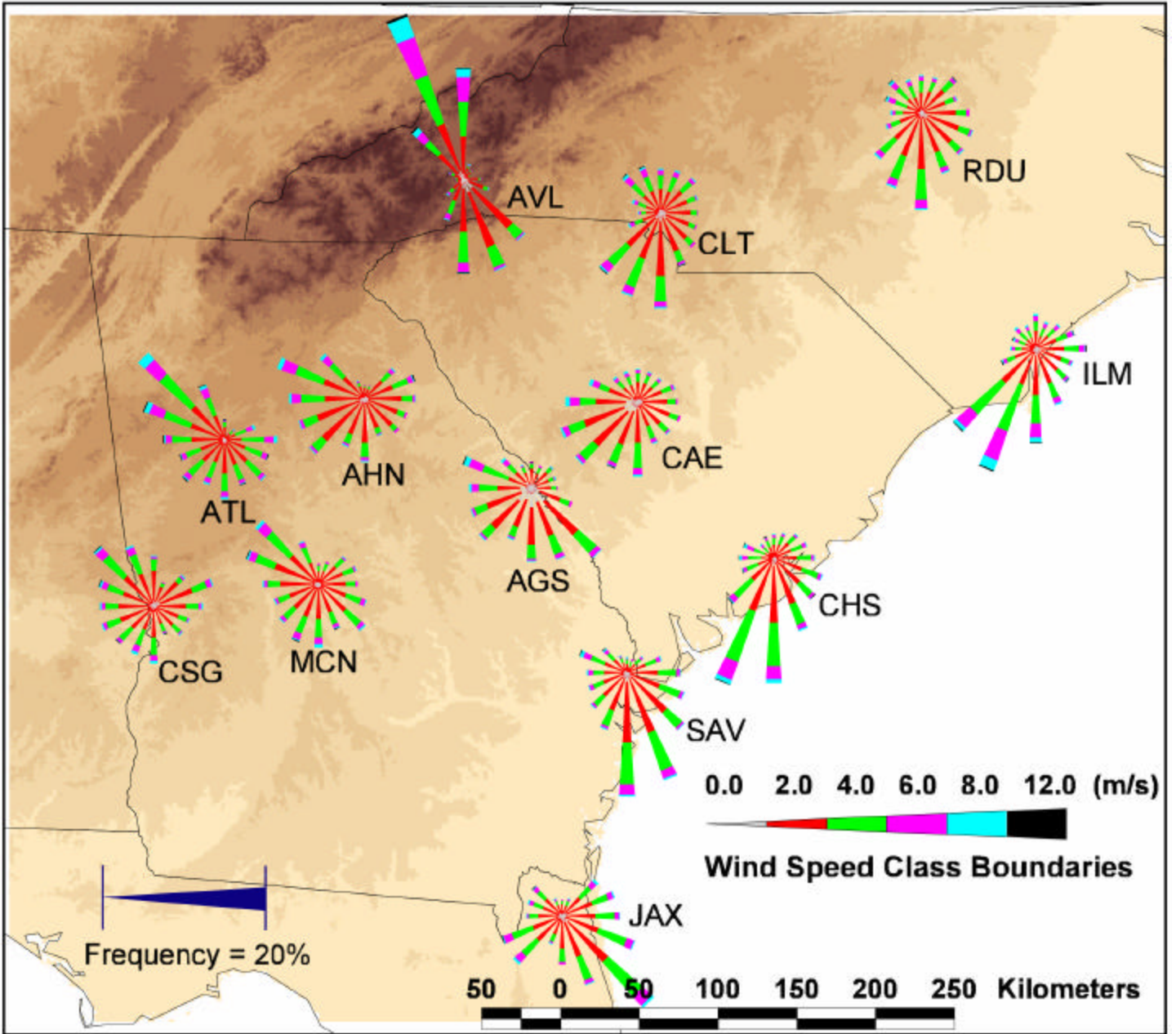


Figure 9. Spring evening (18:00-23:00 LST).

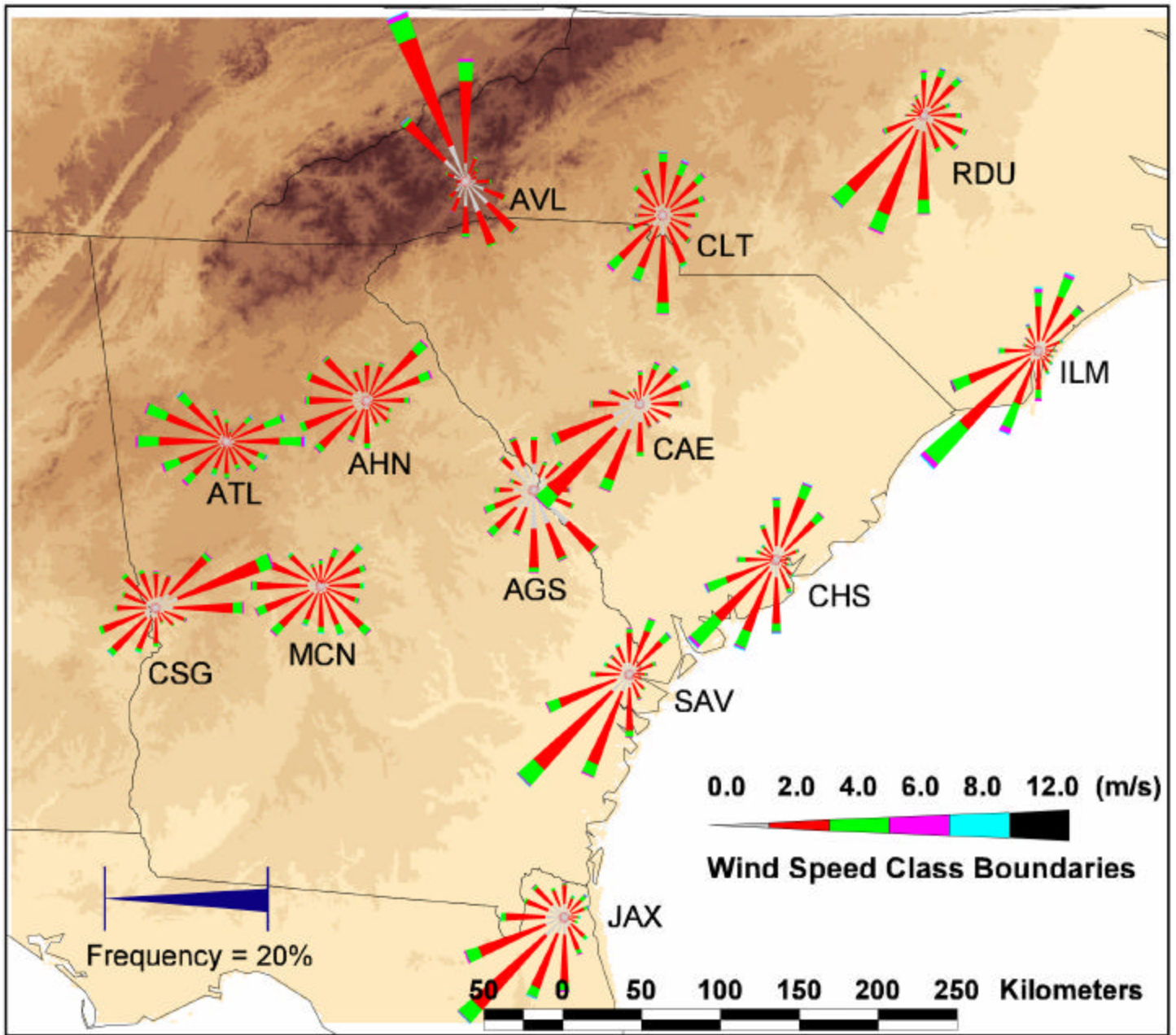


Figure 10. Summer pre-sunrise (00:00-05:00 LST).

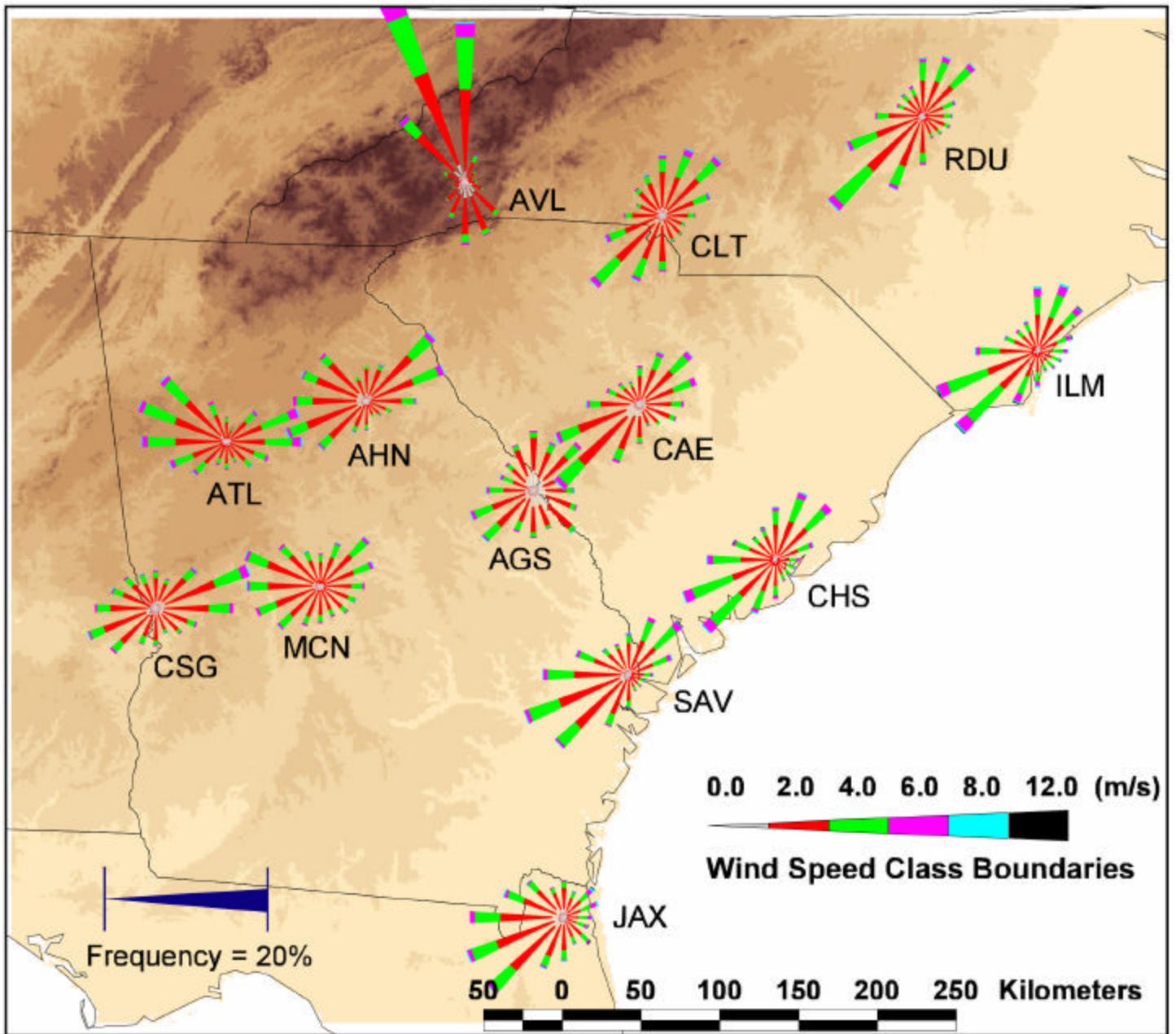


Figure 11. Summer morning (00:06-11:00 LST).

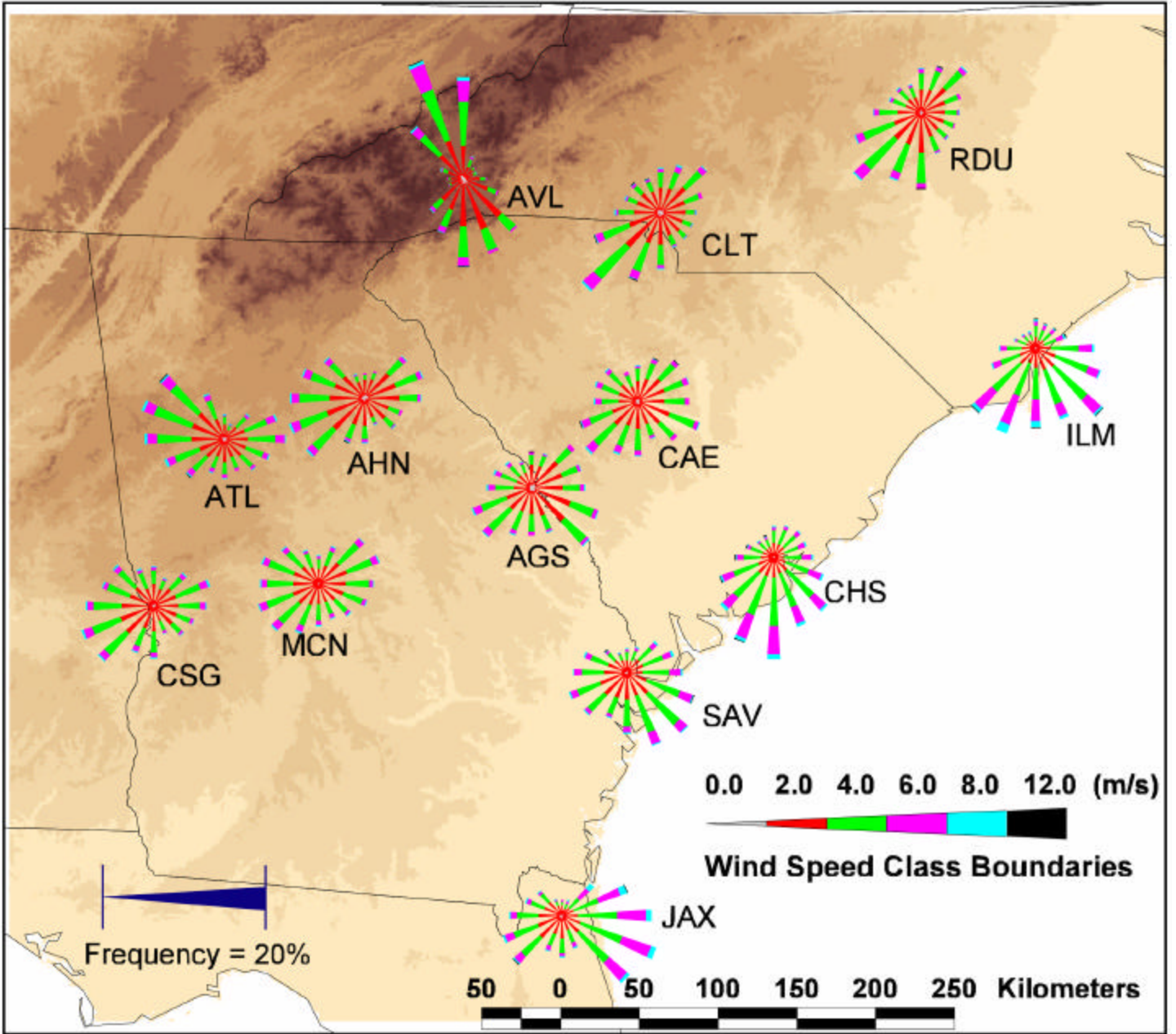


Figure 12. Summer afternoon (12:00-17:00 LST).

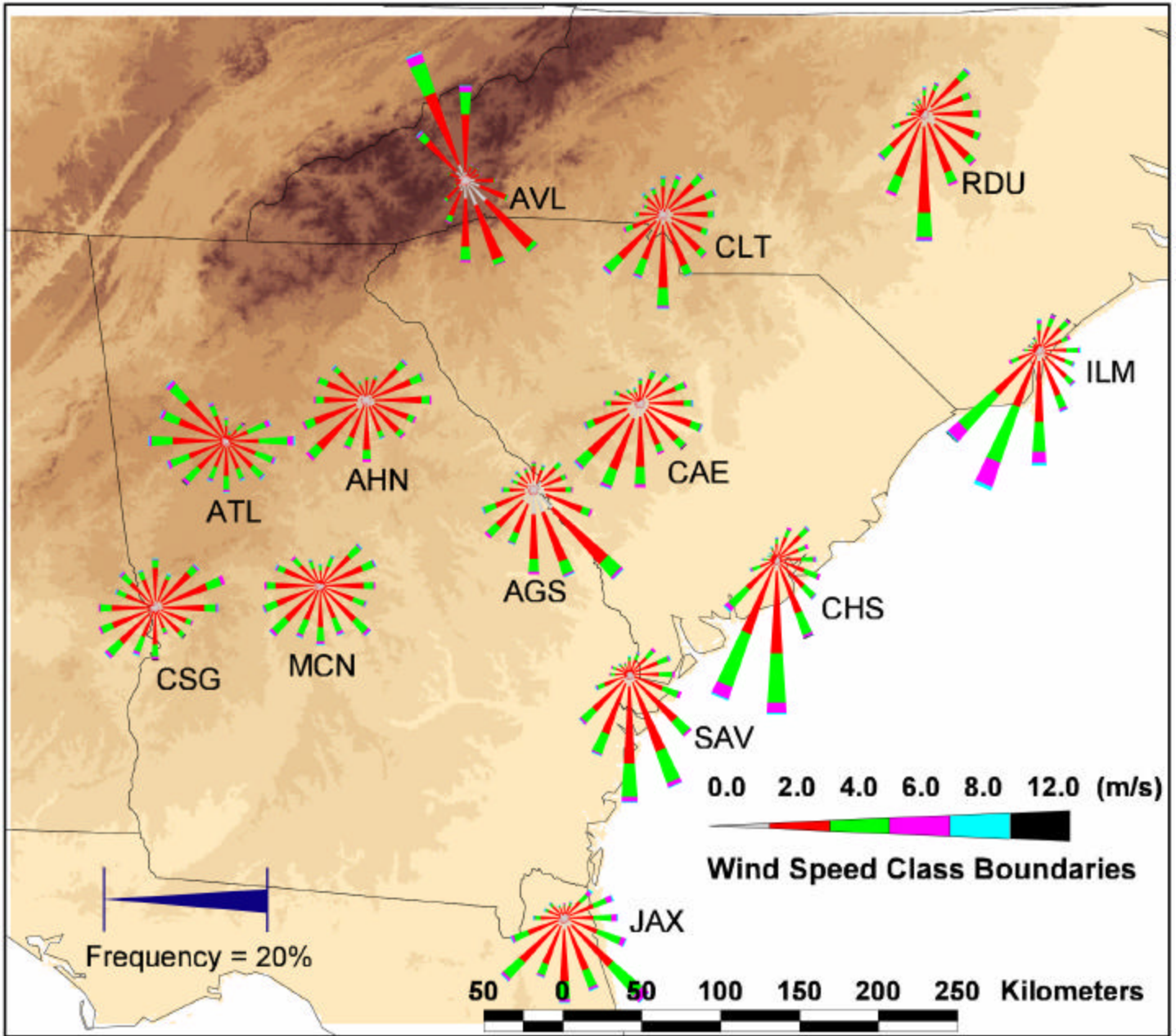


Figure 13. Summer evening (18:00-23:00 LST).

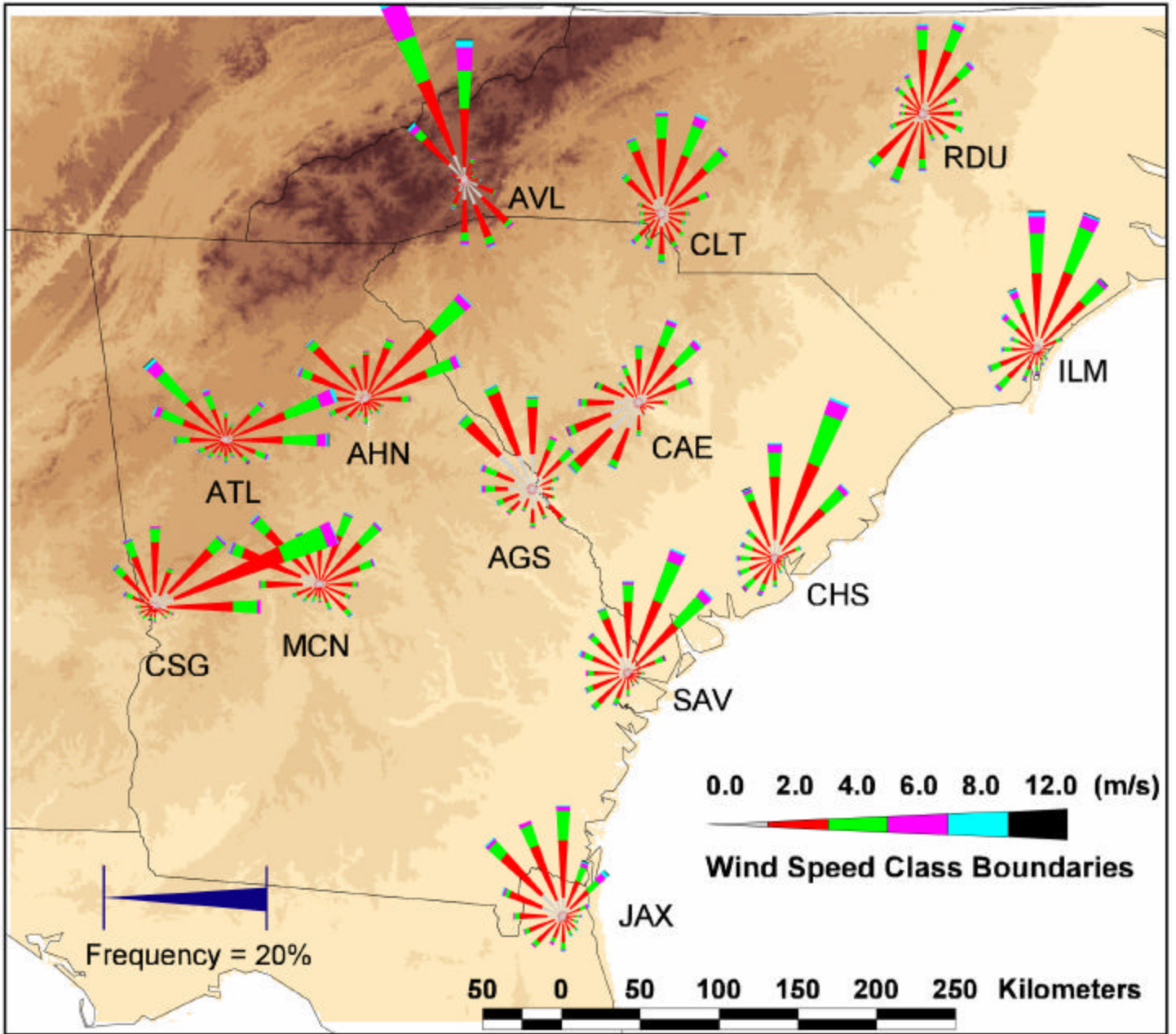


Figure 14. Autumn pre-sunrise (00:00-05:00 LST).

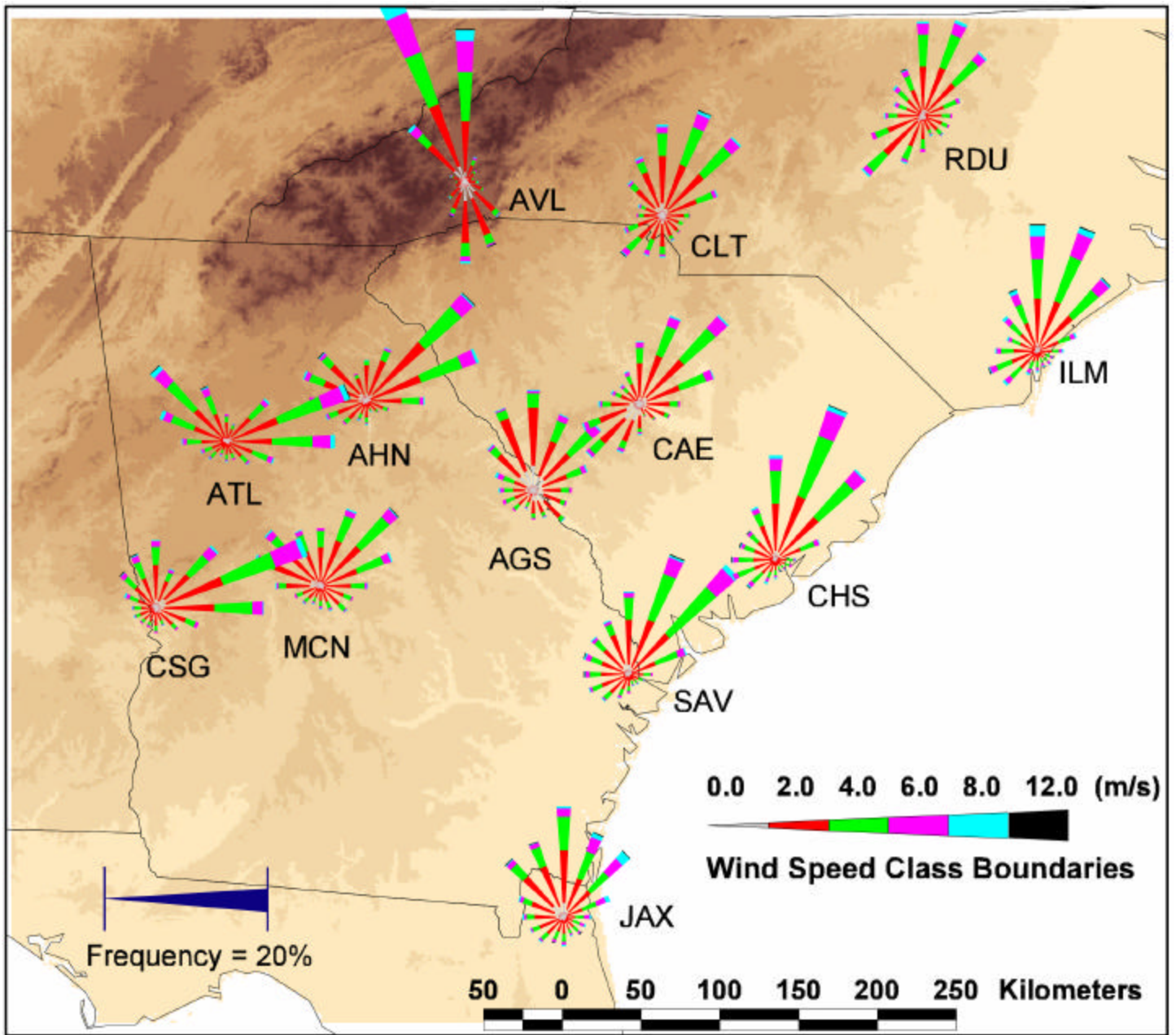


Figure 15. Autumn morning (00:06-11:00 LST).

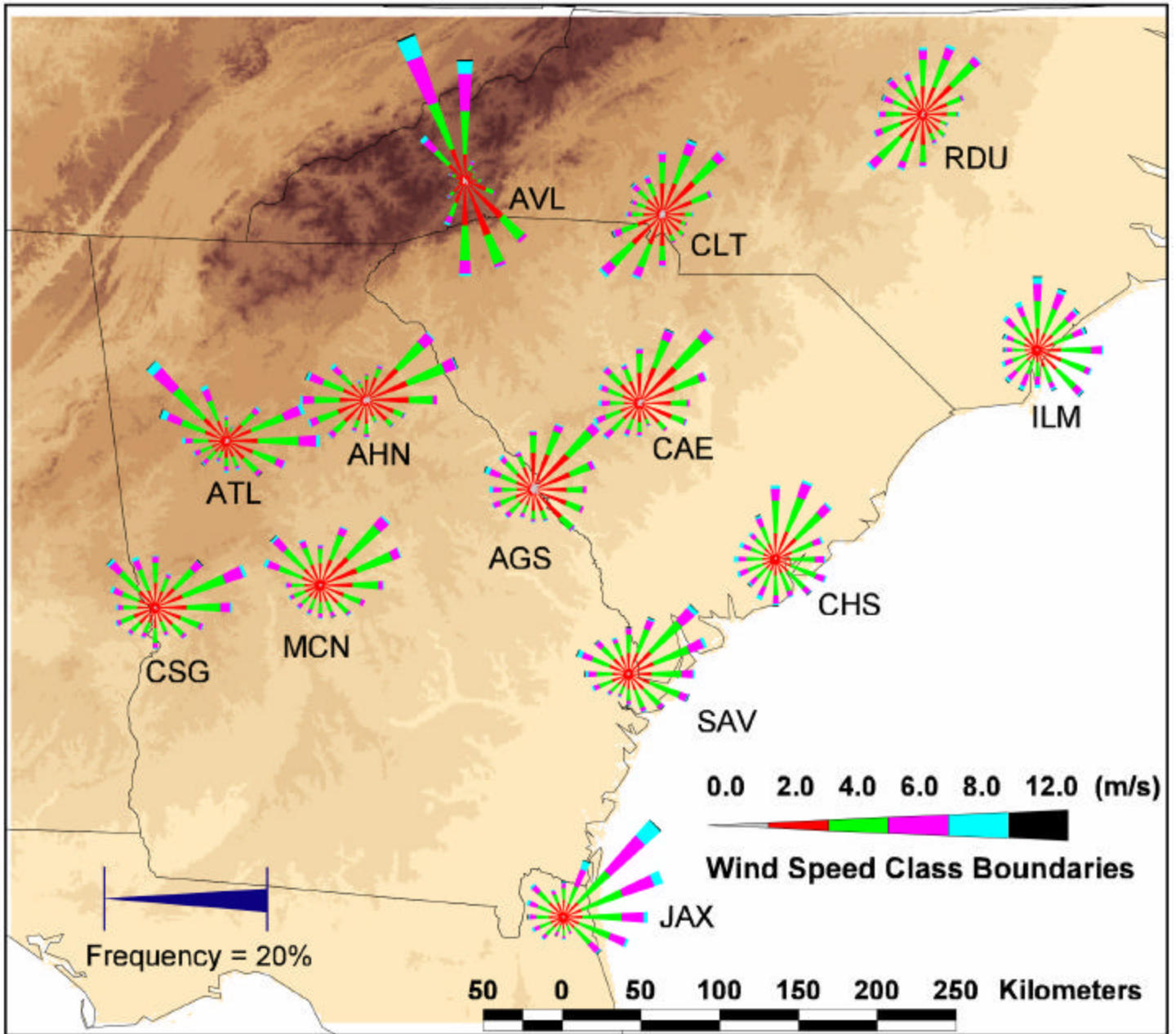


Figure 16. Autumn afternoon (12:00-17:00 LST).

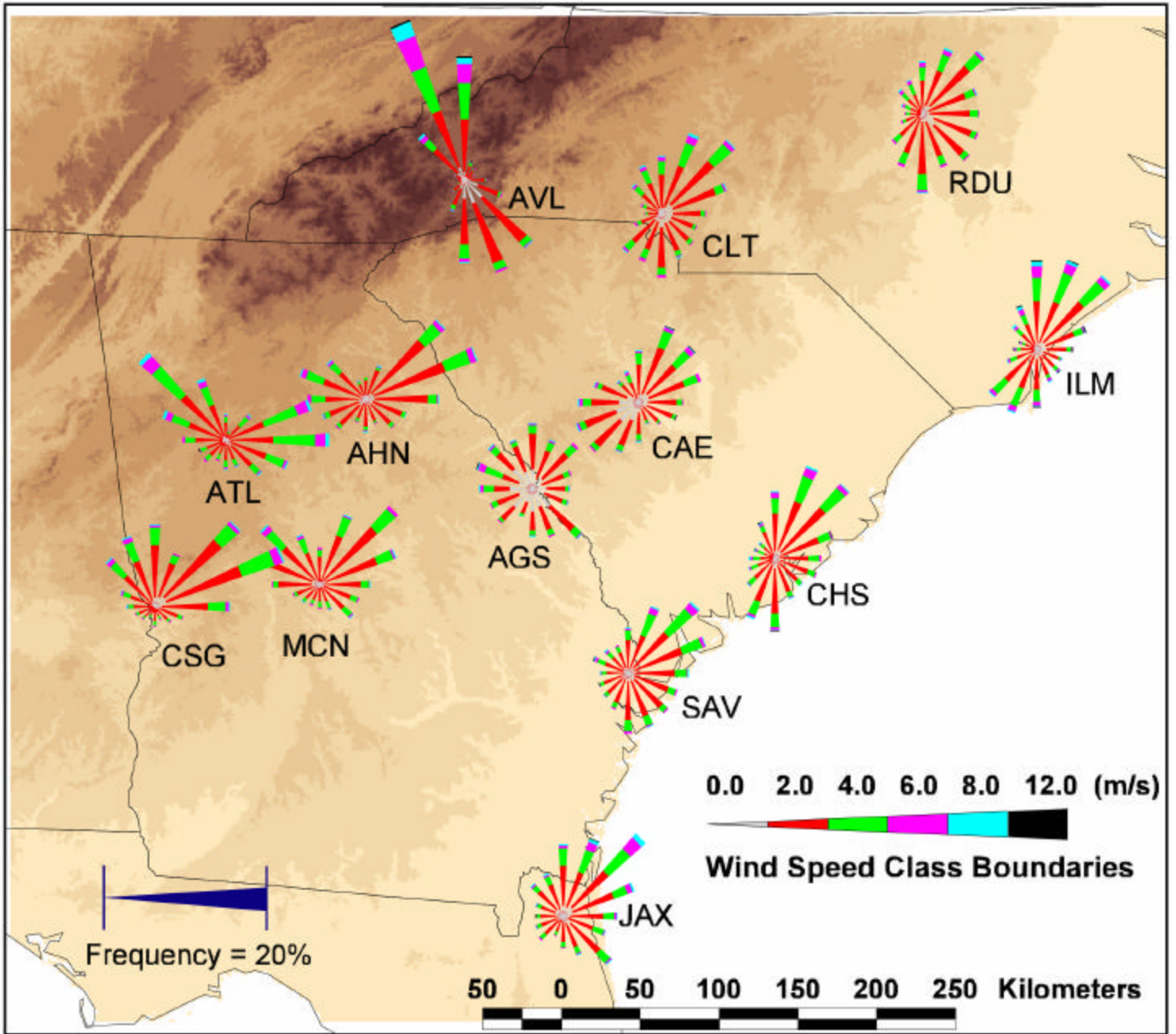


Figure 17. Autumn evening (18:00-23:00 LST).

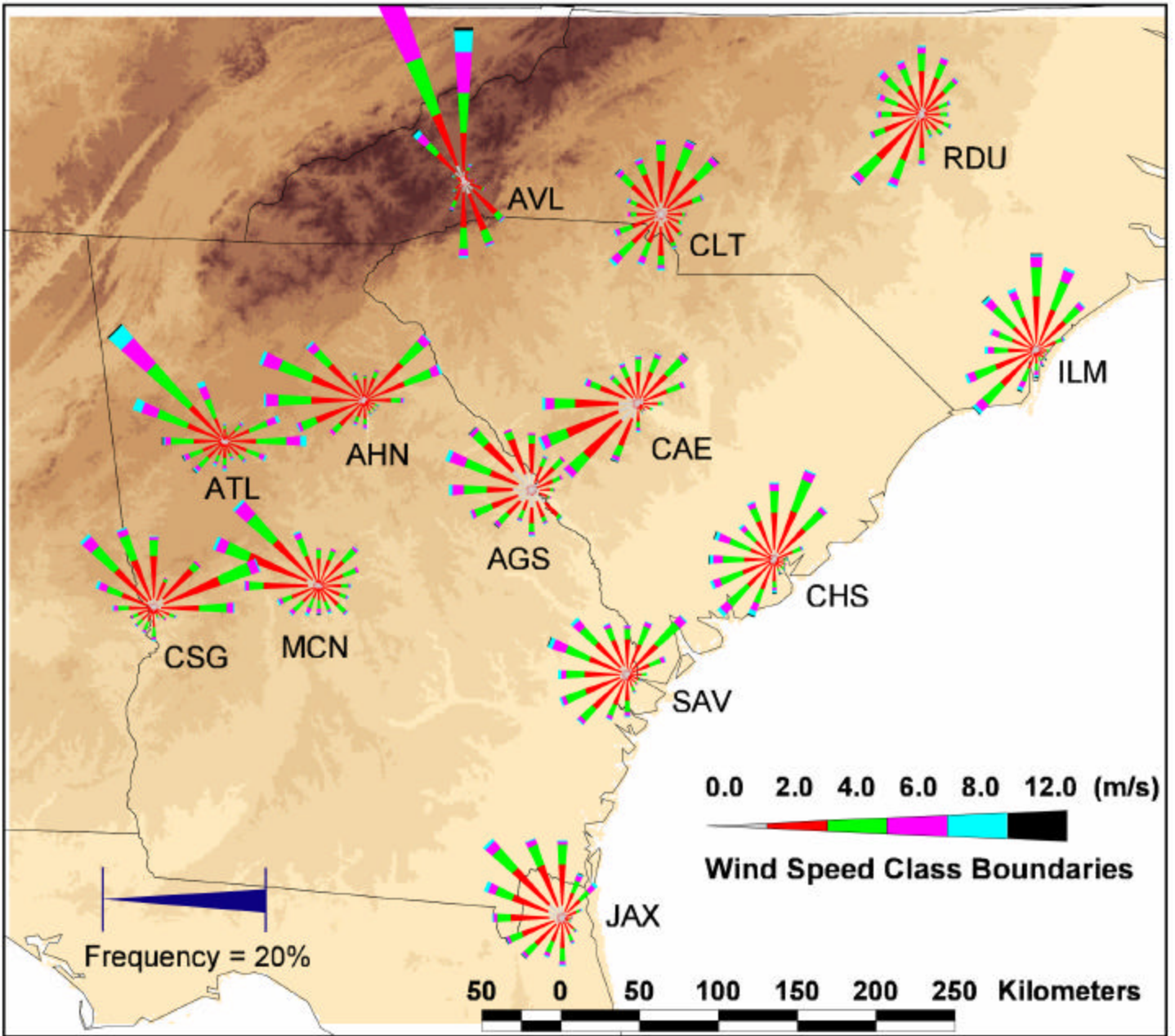


Figure 18. Winter pre-sunrise (00:00-05:00 LST).

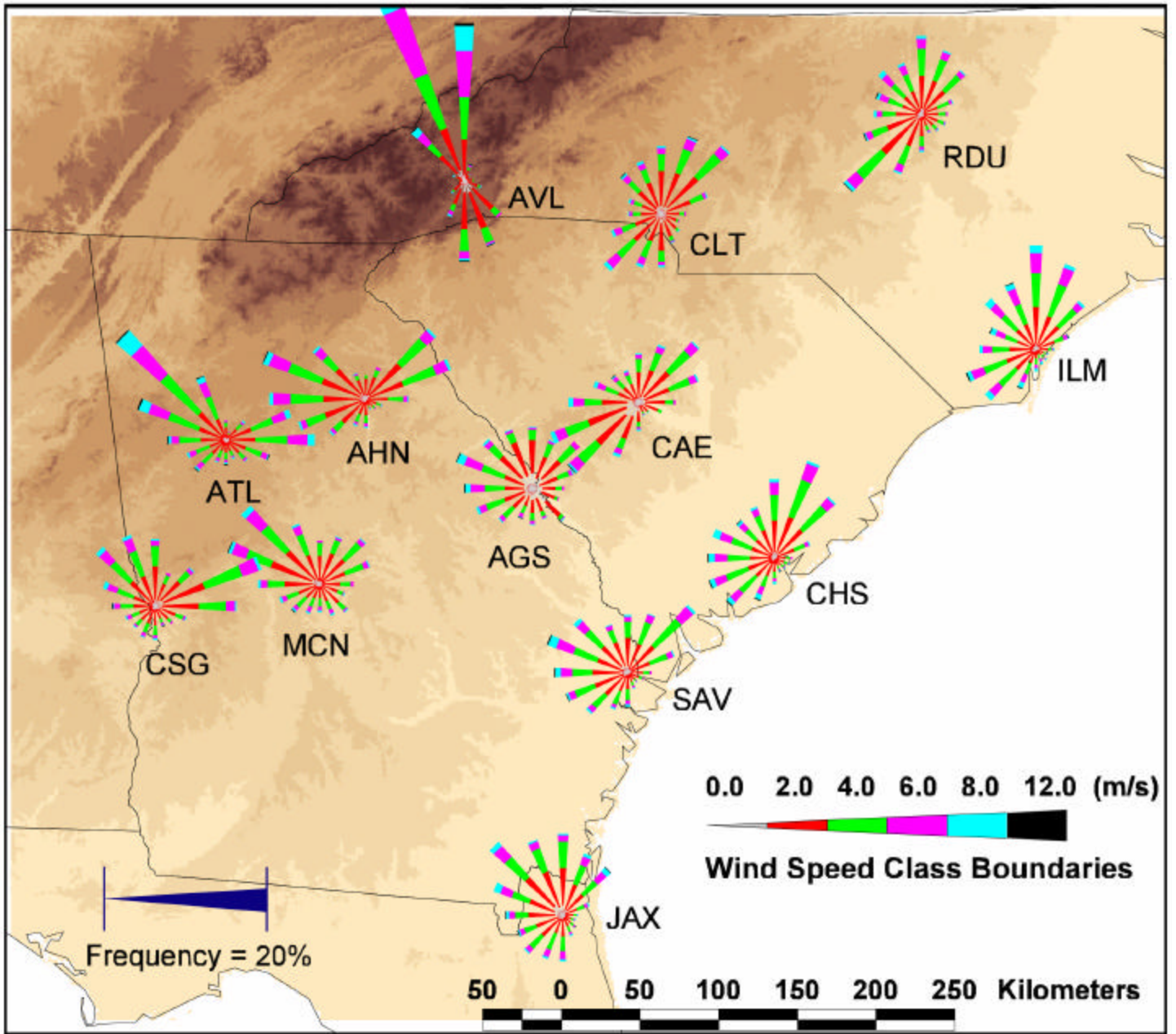


Figure 19. Winter morning (00:06-11:00 LST).

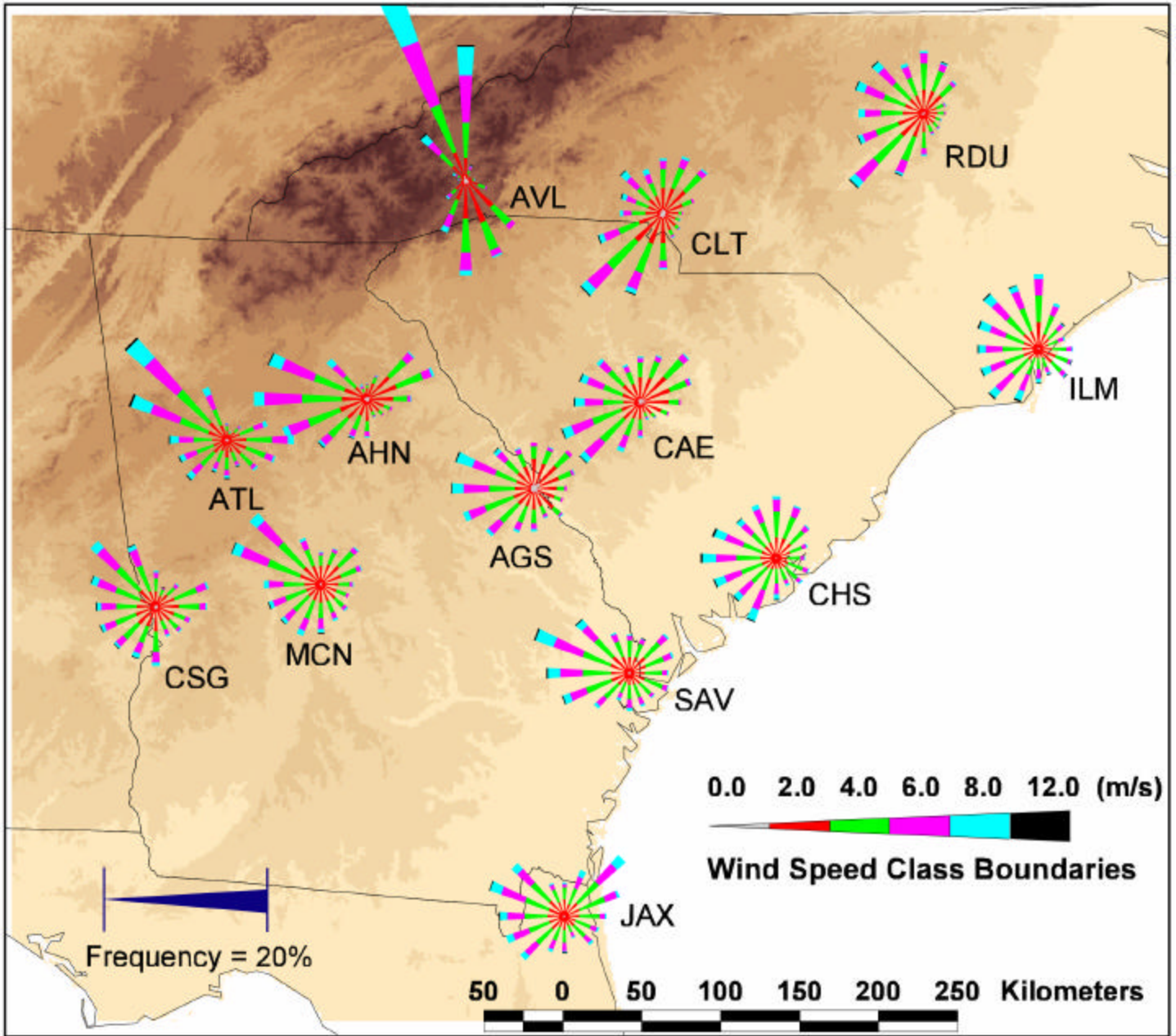


Figure 20. Winter afternoon (12:00-17:00 LST).

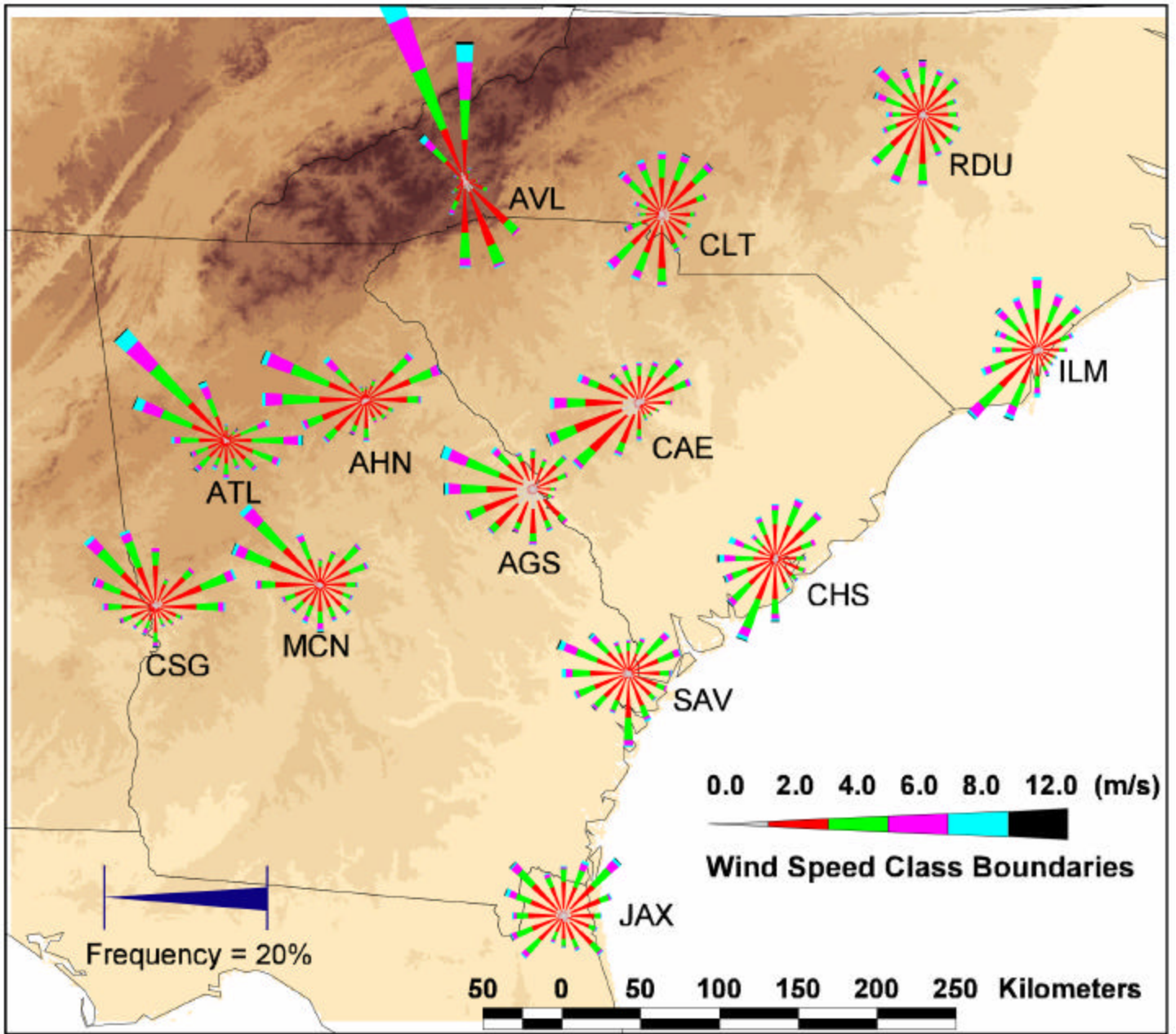


Figure 21. Winter evening (18:00-23:00 LST).

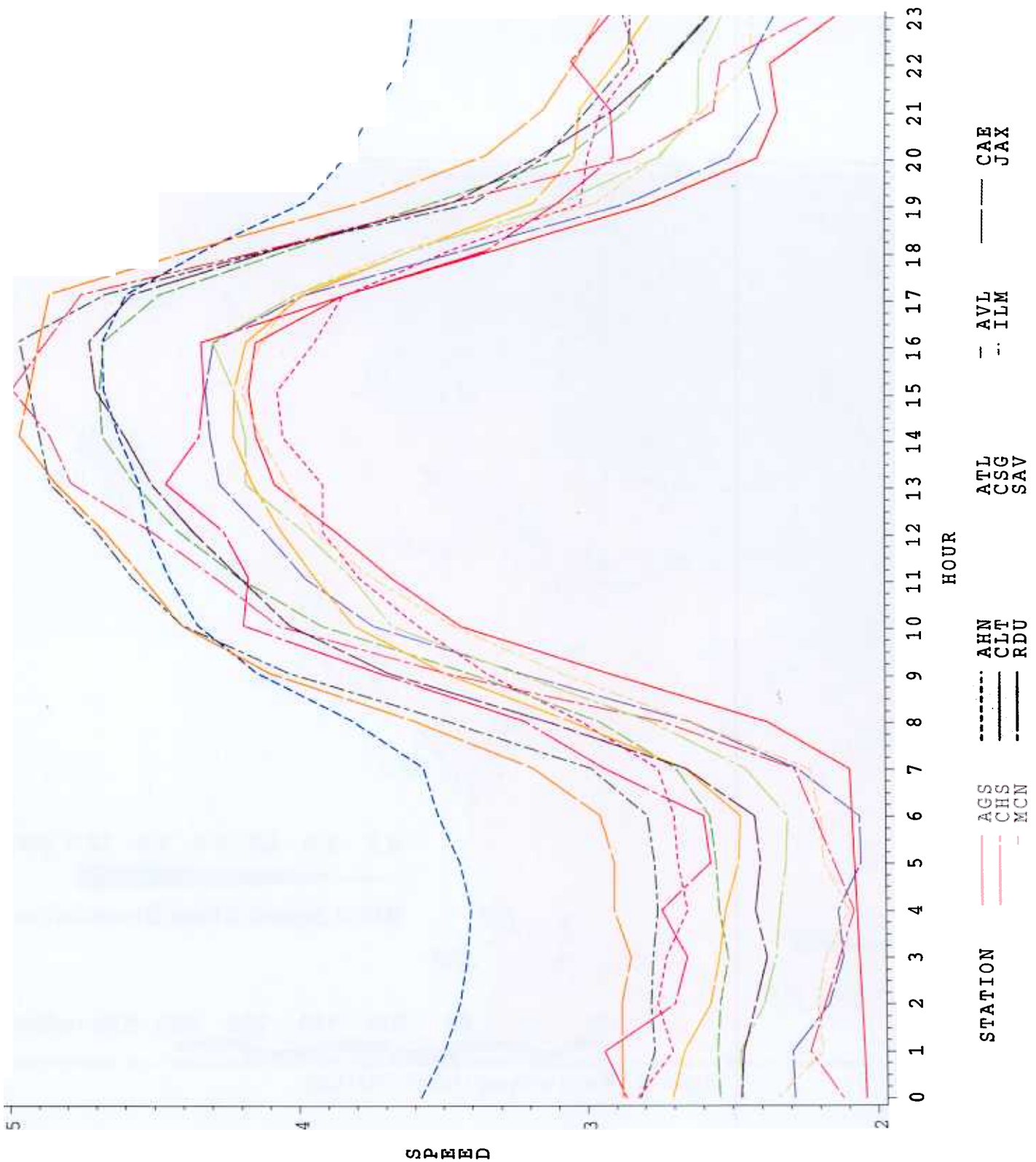


Fig. 22. All stations wind speed (m/s) 8

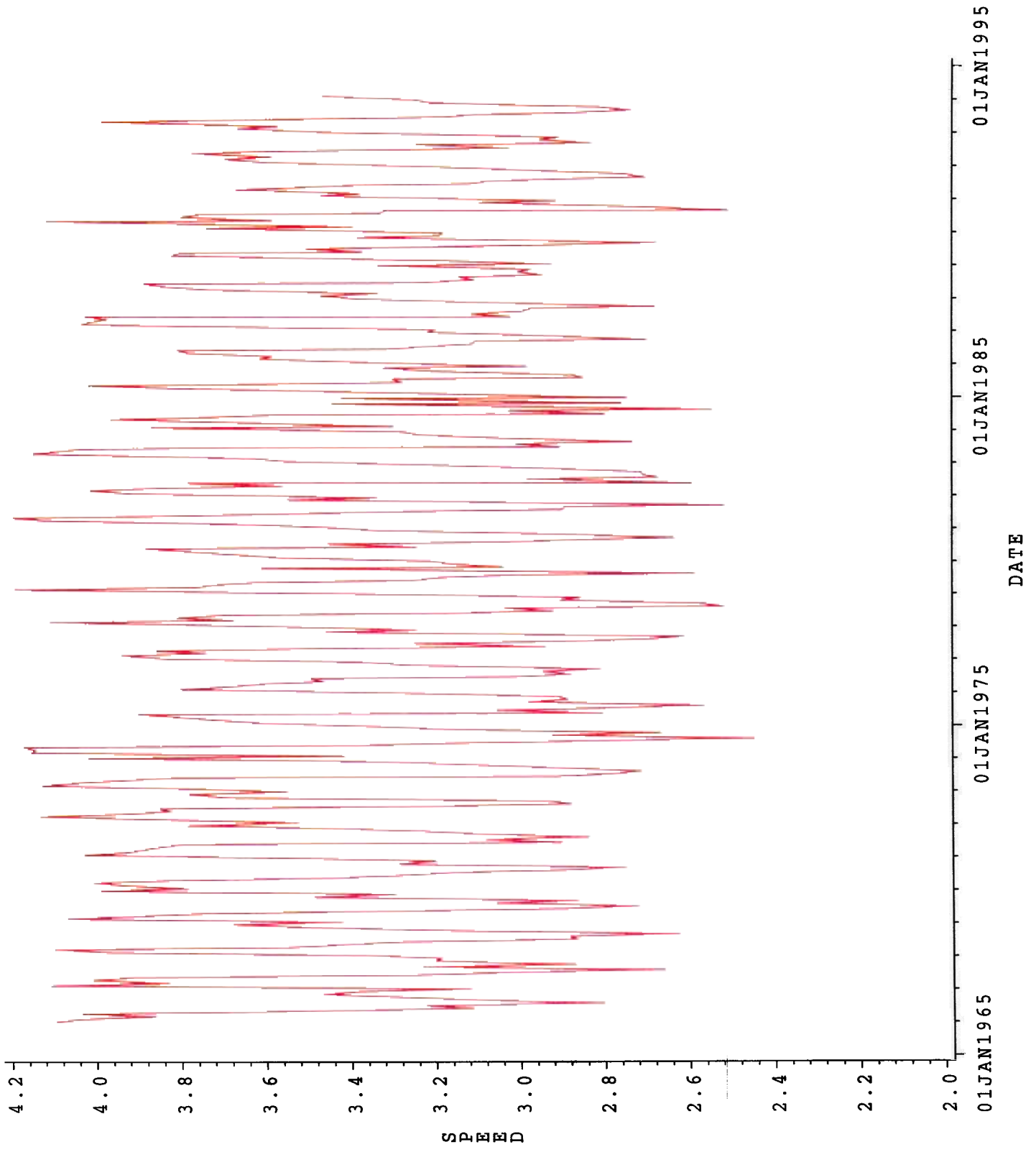


Fig. 23 Ensemble average wind speed (m/s)₃₉

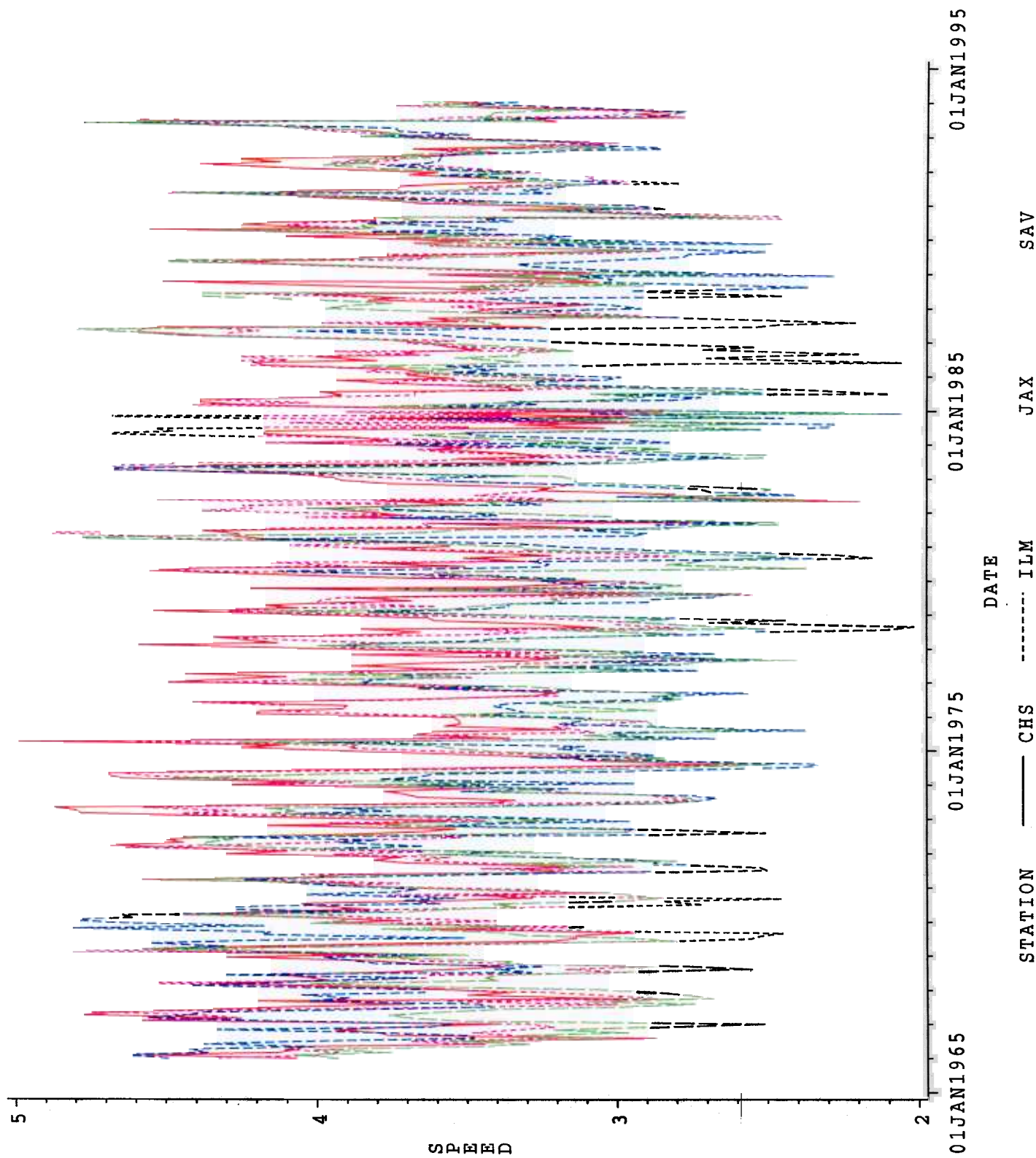


Fig. 24. Coastal stations wind speed (m/s)

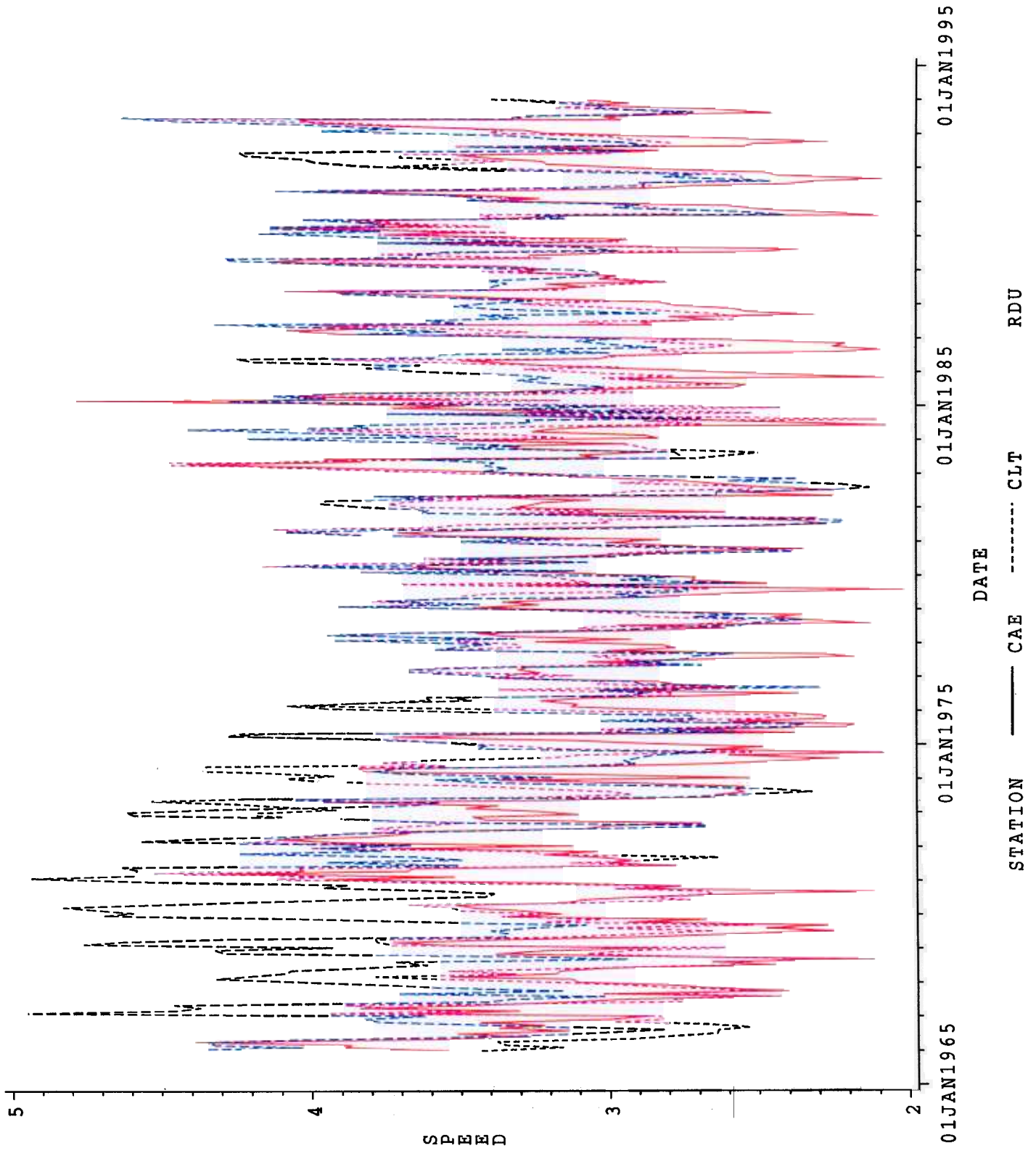


Fig. 25. Piedmont stations wind speed (m/s)
41

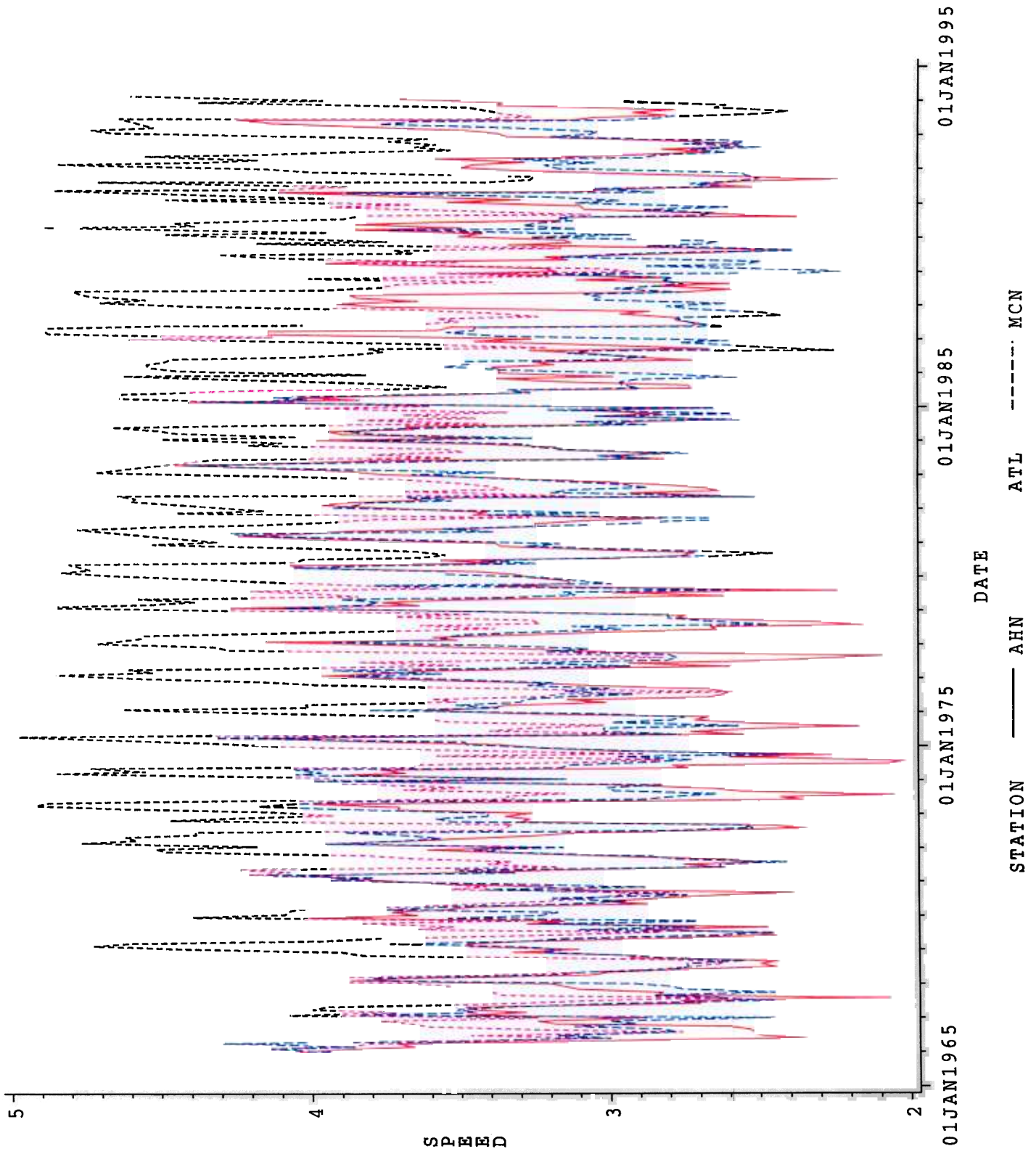


Fig 26. Southern Appalachians stations wind speed (m/s)

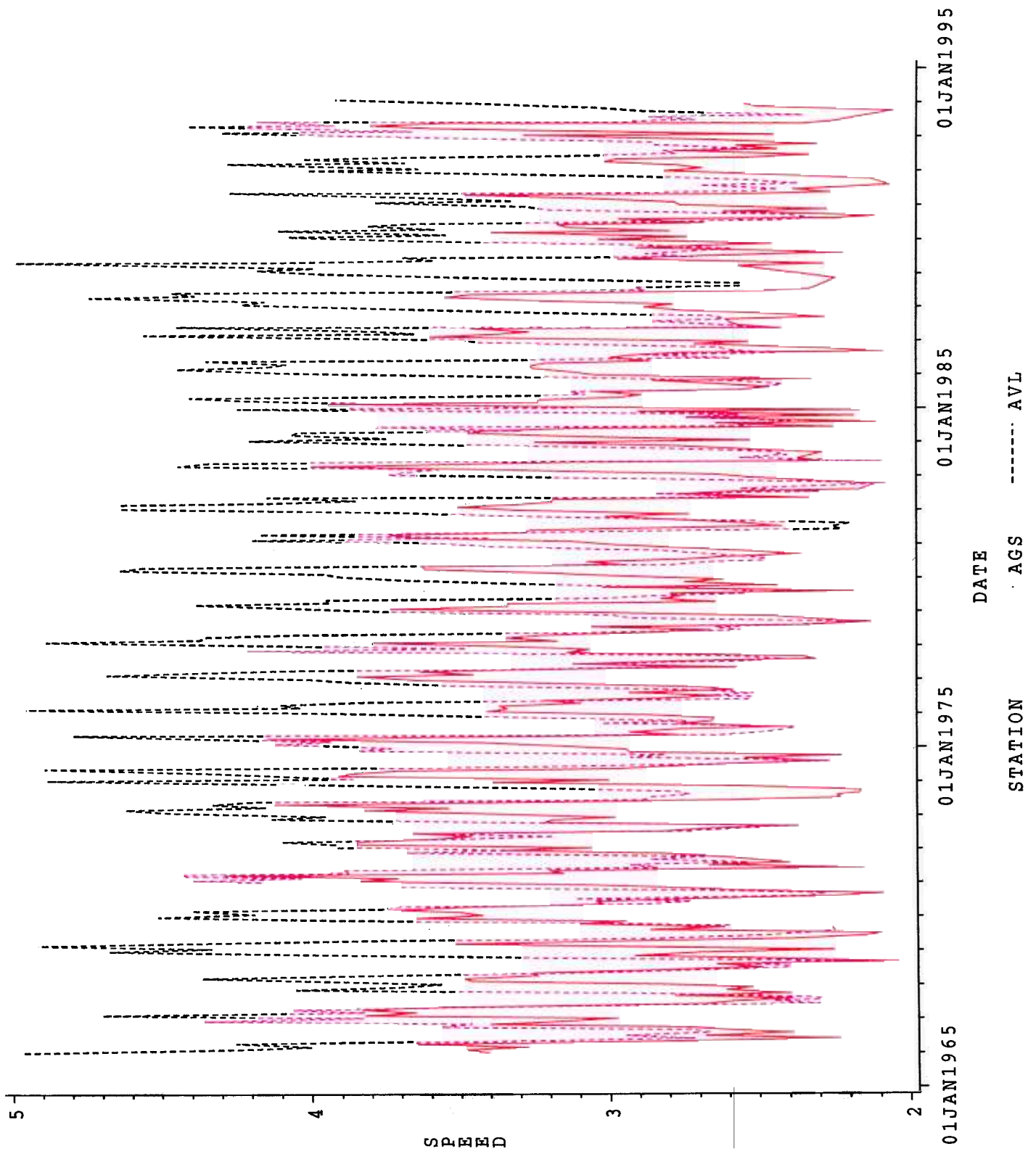


Fig. 27 Remaining stations wind speed (m/s)
43

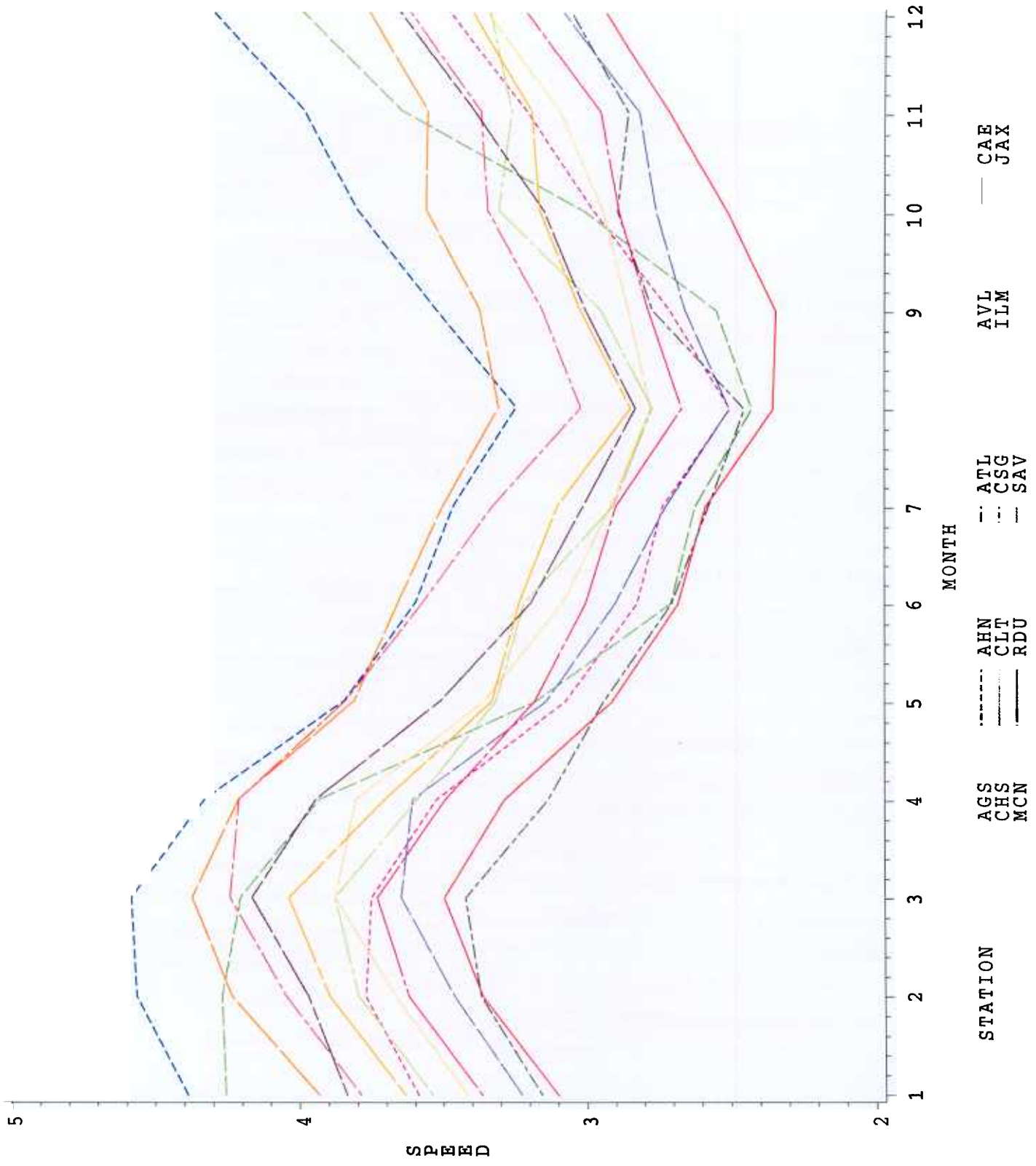
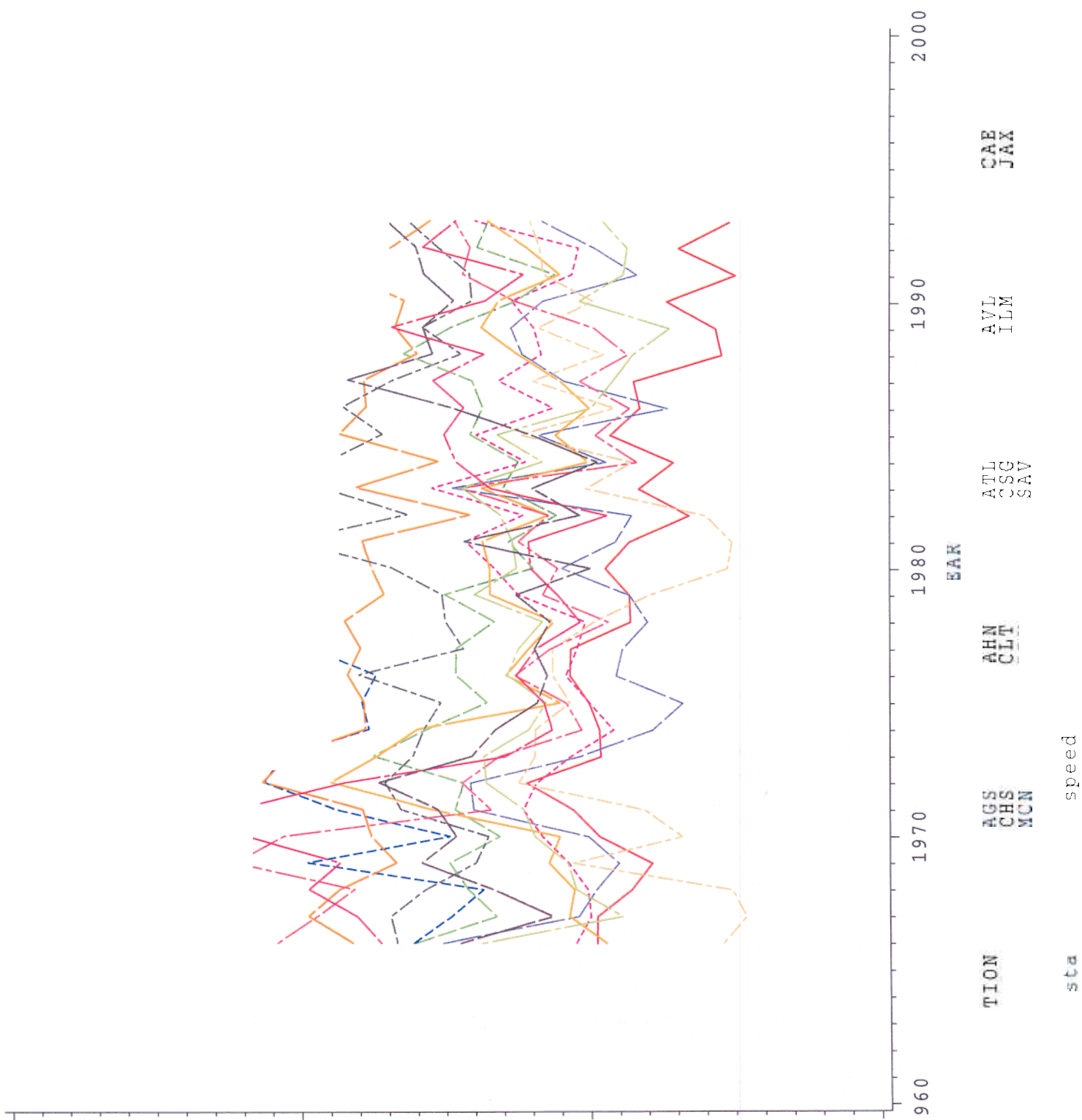


Fig. 28. All Southeast stations wind speed (m/s)



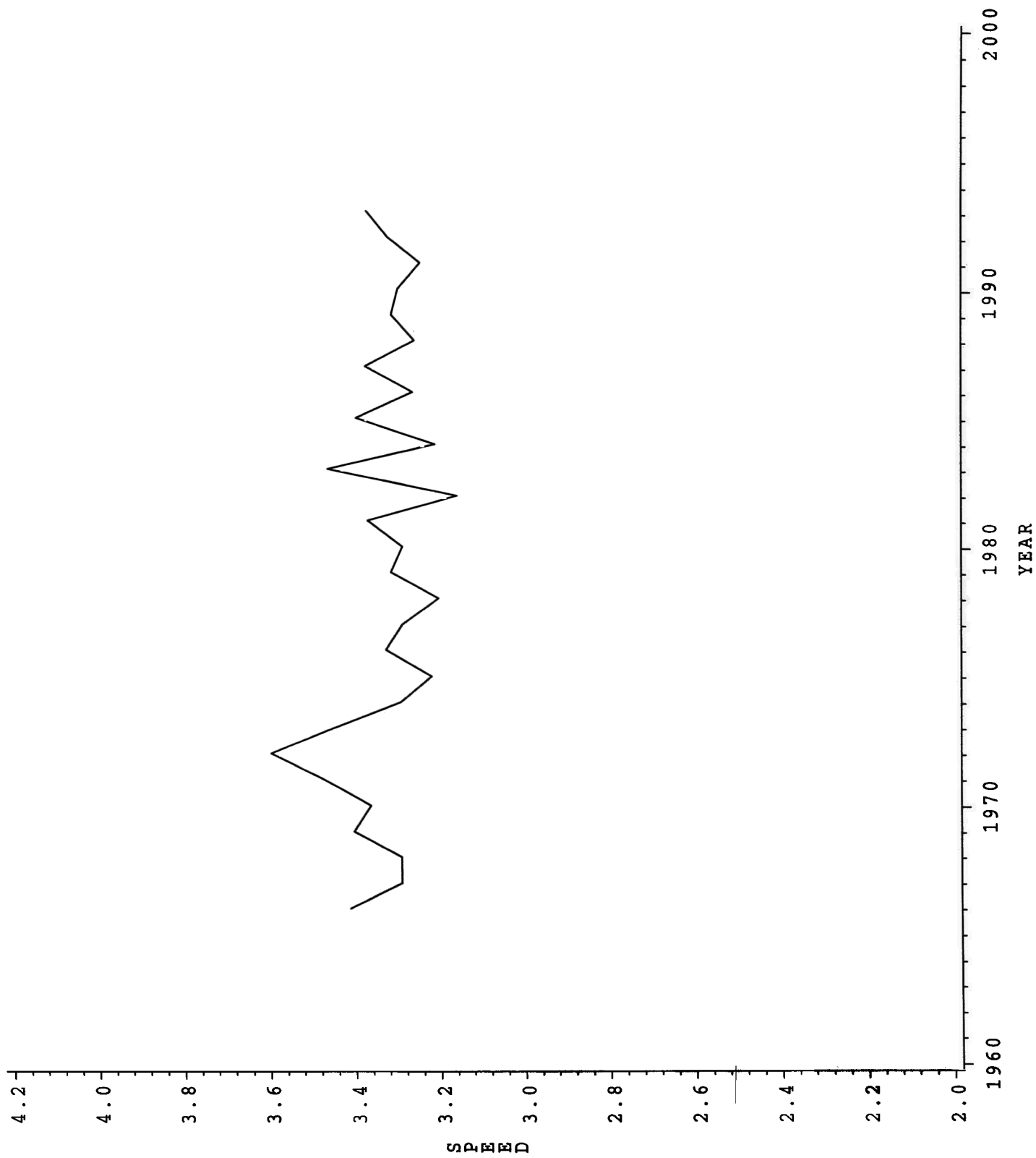


Fig 30. Ensemble average wind speed (m/s) 6

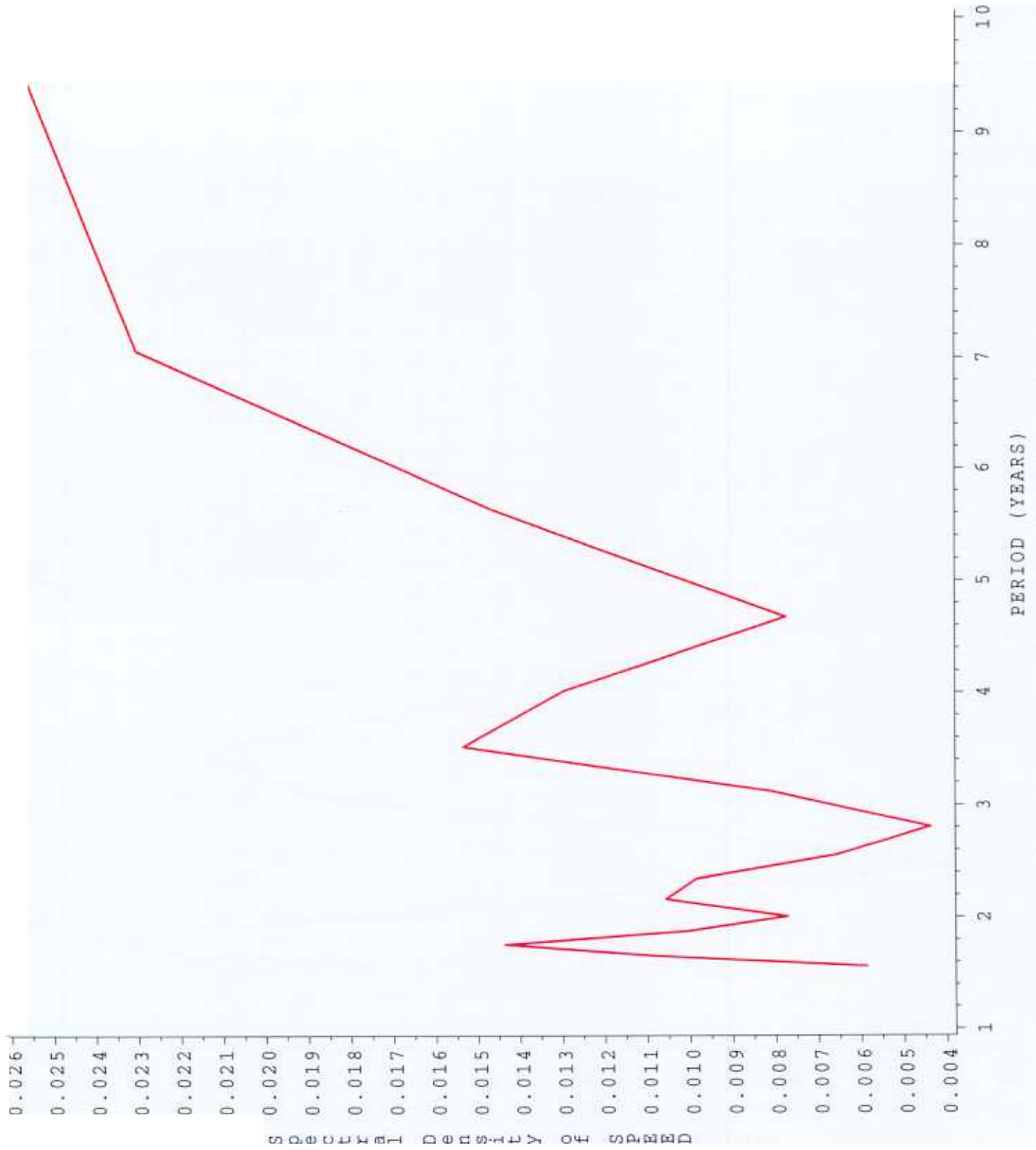


Fig. 31. Spectral density of averaged speeds for all stations

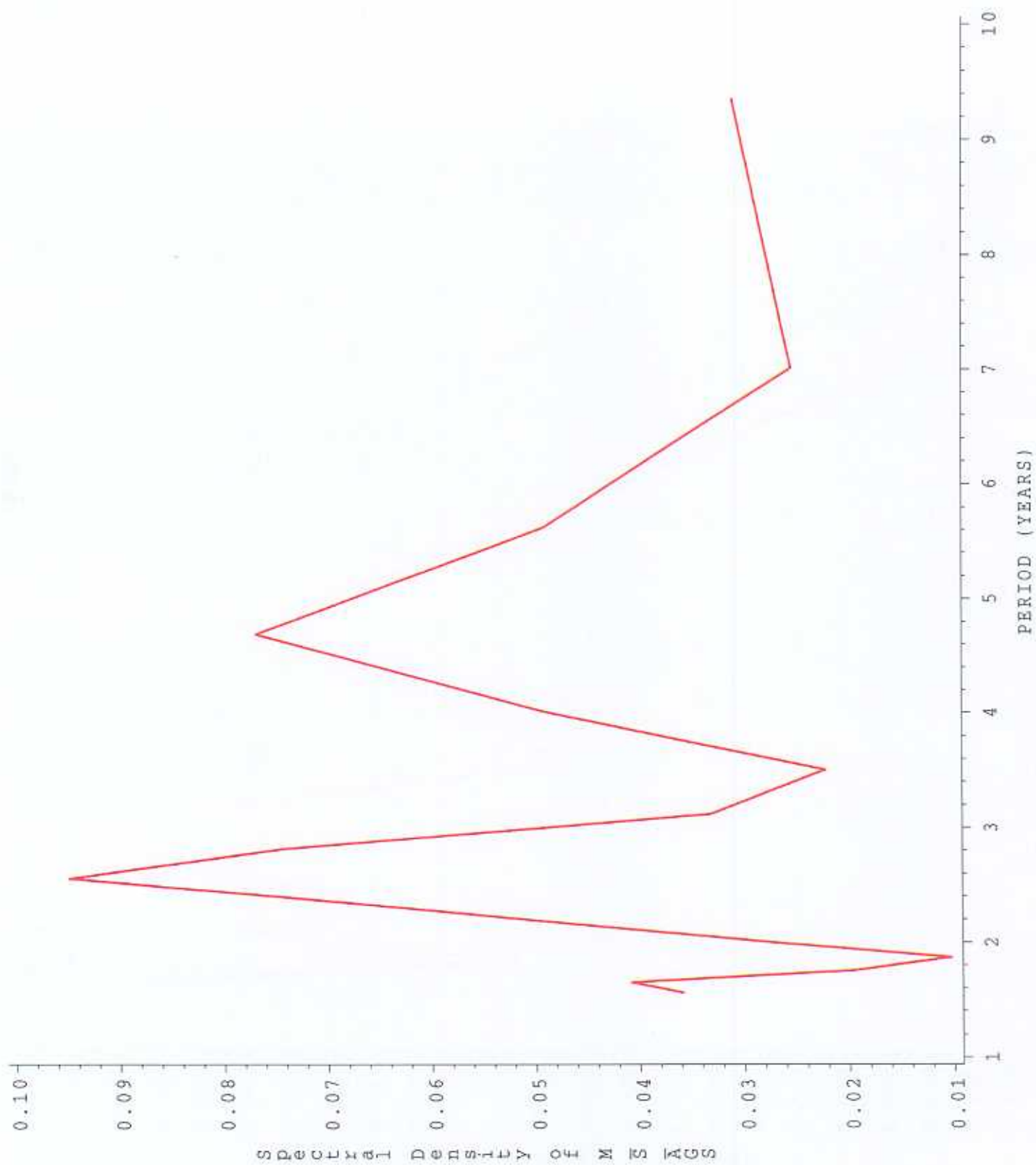


Fig. 32. Spectral density of wind speed for AGS

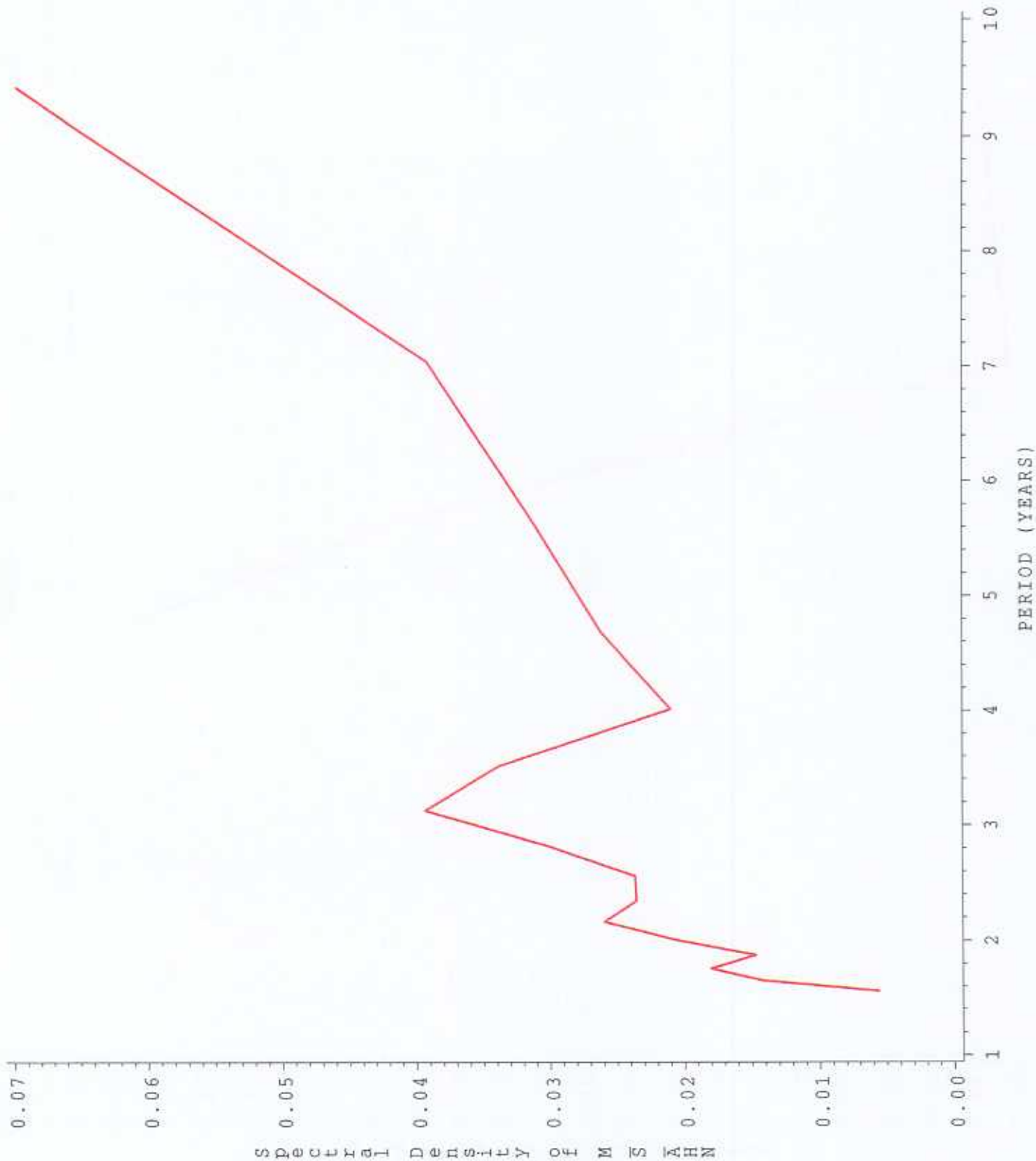


Fig. 33. Spectral density of wind speed for AN₄₉

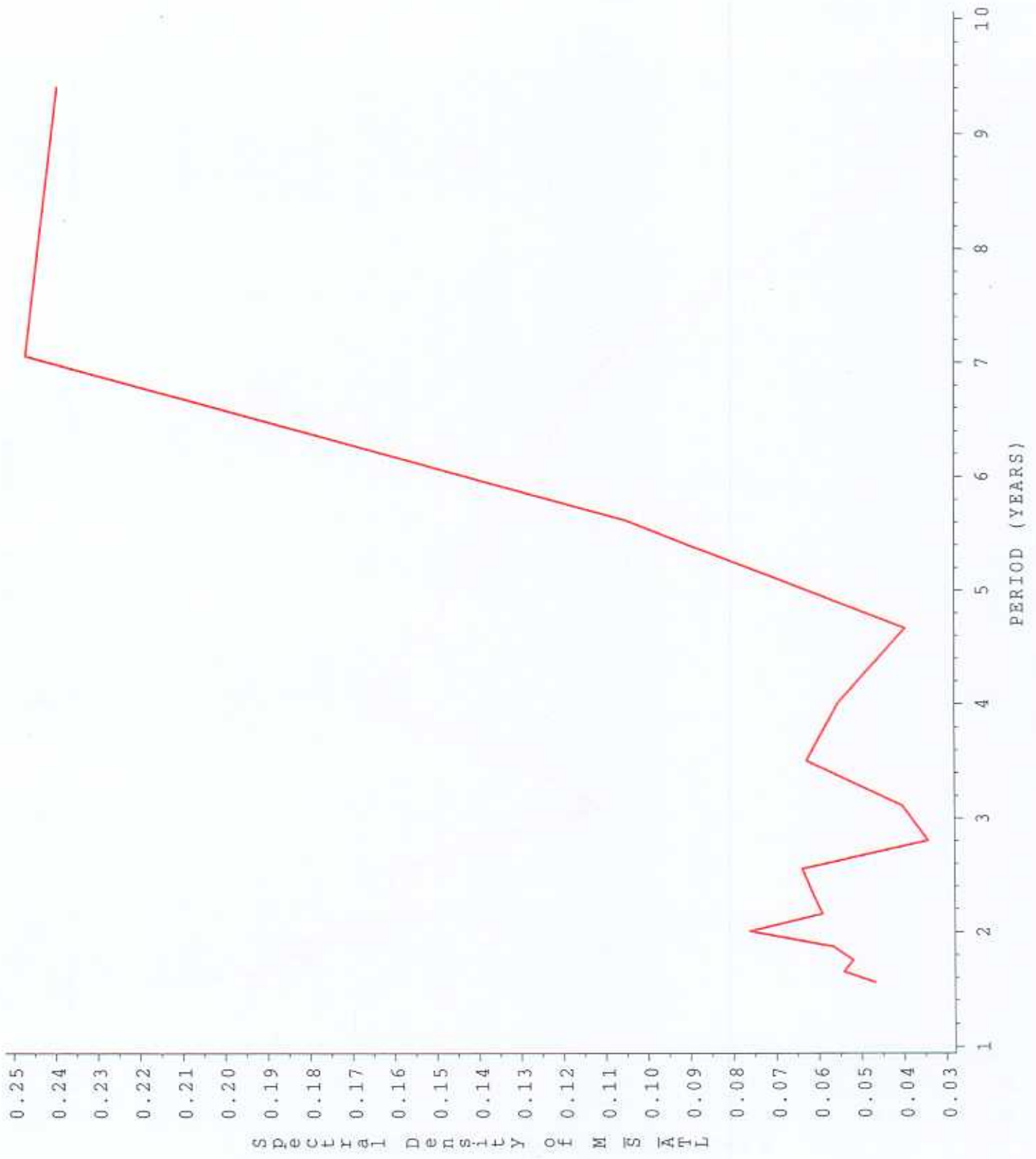


Fig. 34. Spectral density of wind speed for ATL

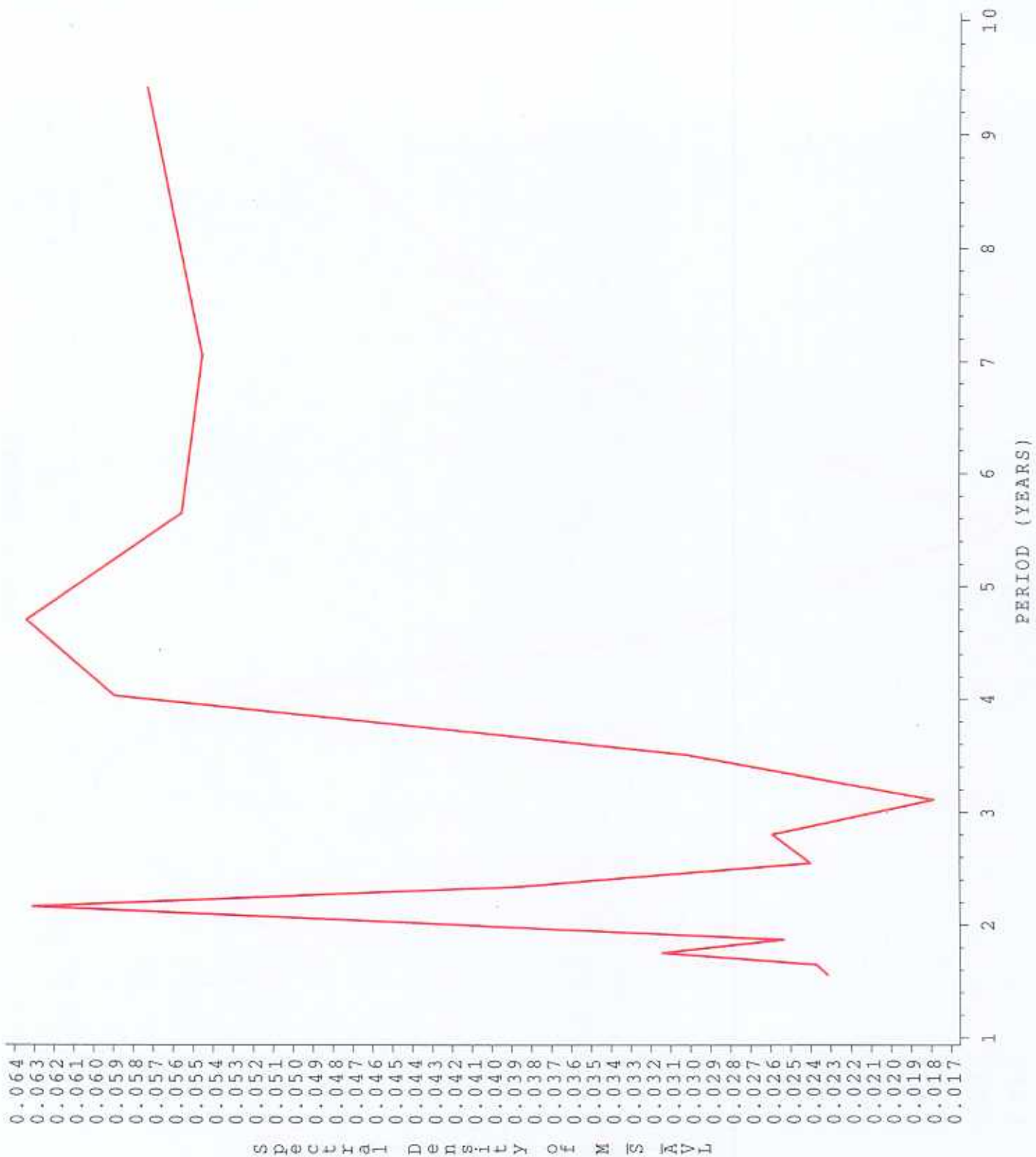


Fig. 35. Spectral density of wind speed for AVL₅₁

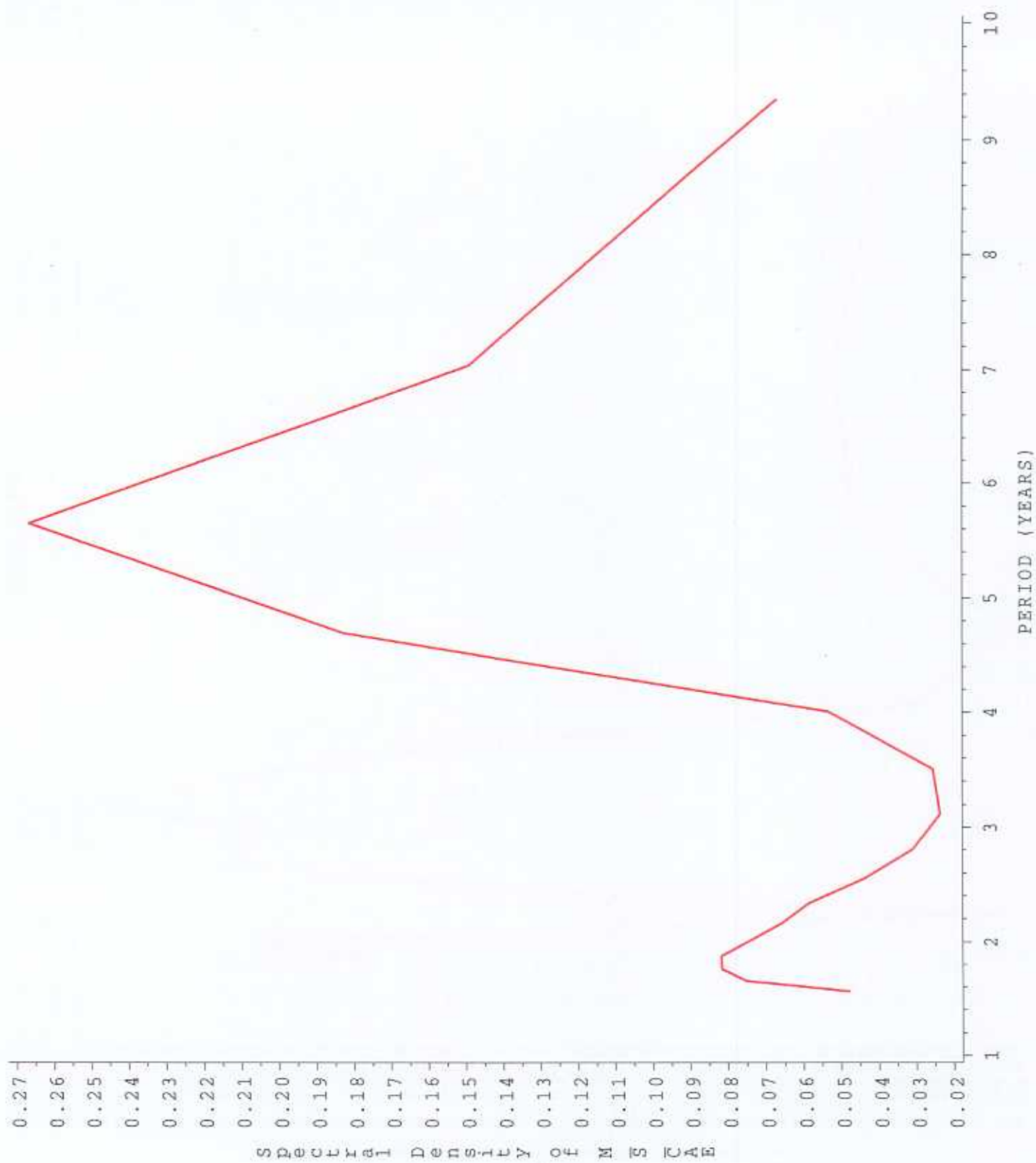


Fig. 36. Spectral density of wind speed for CAE

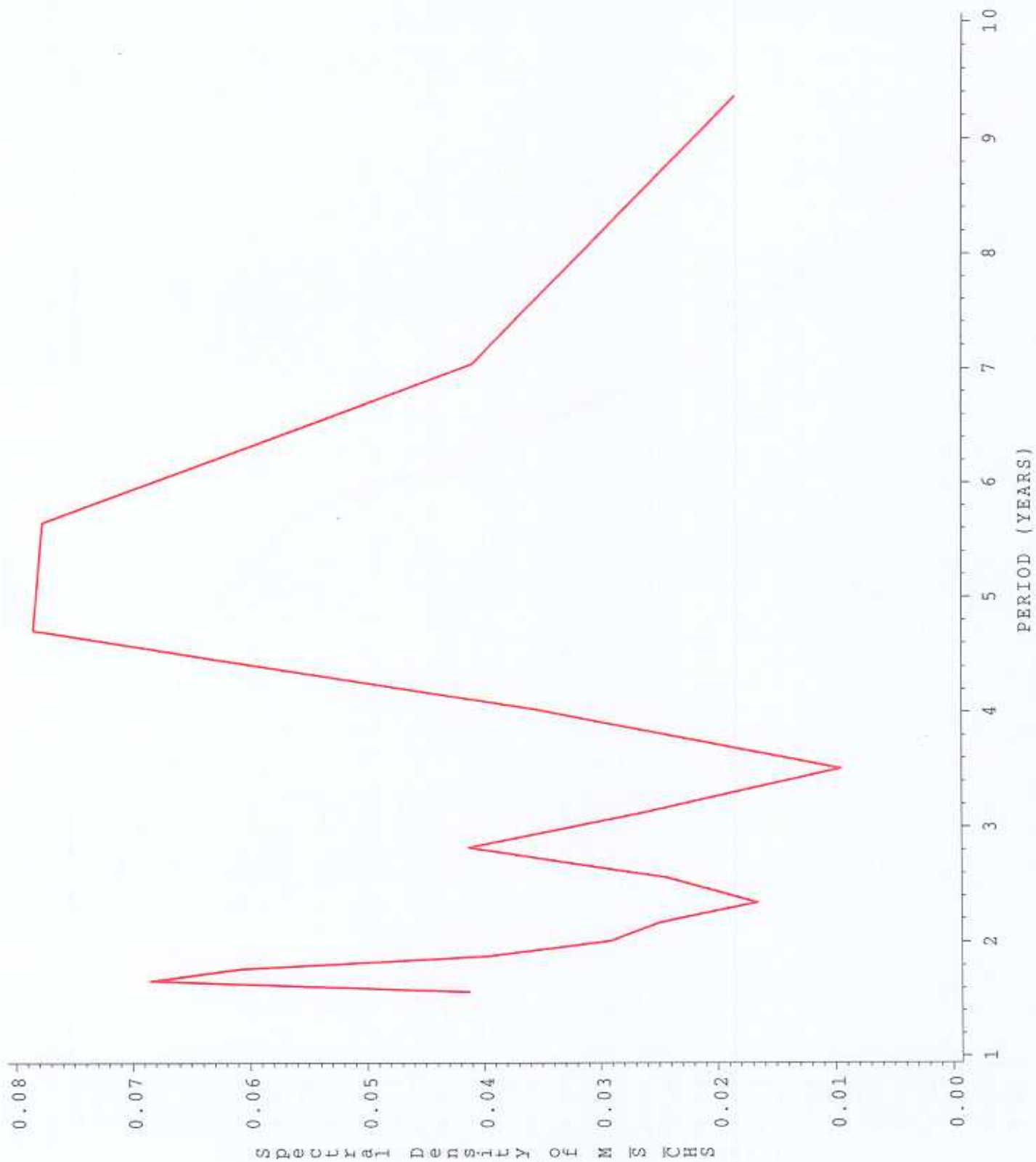


Fig. 37. Spectral density of wind speed for CHS₅₃

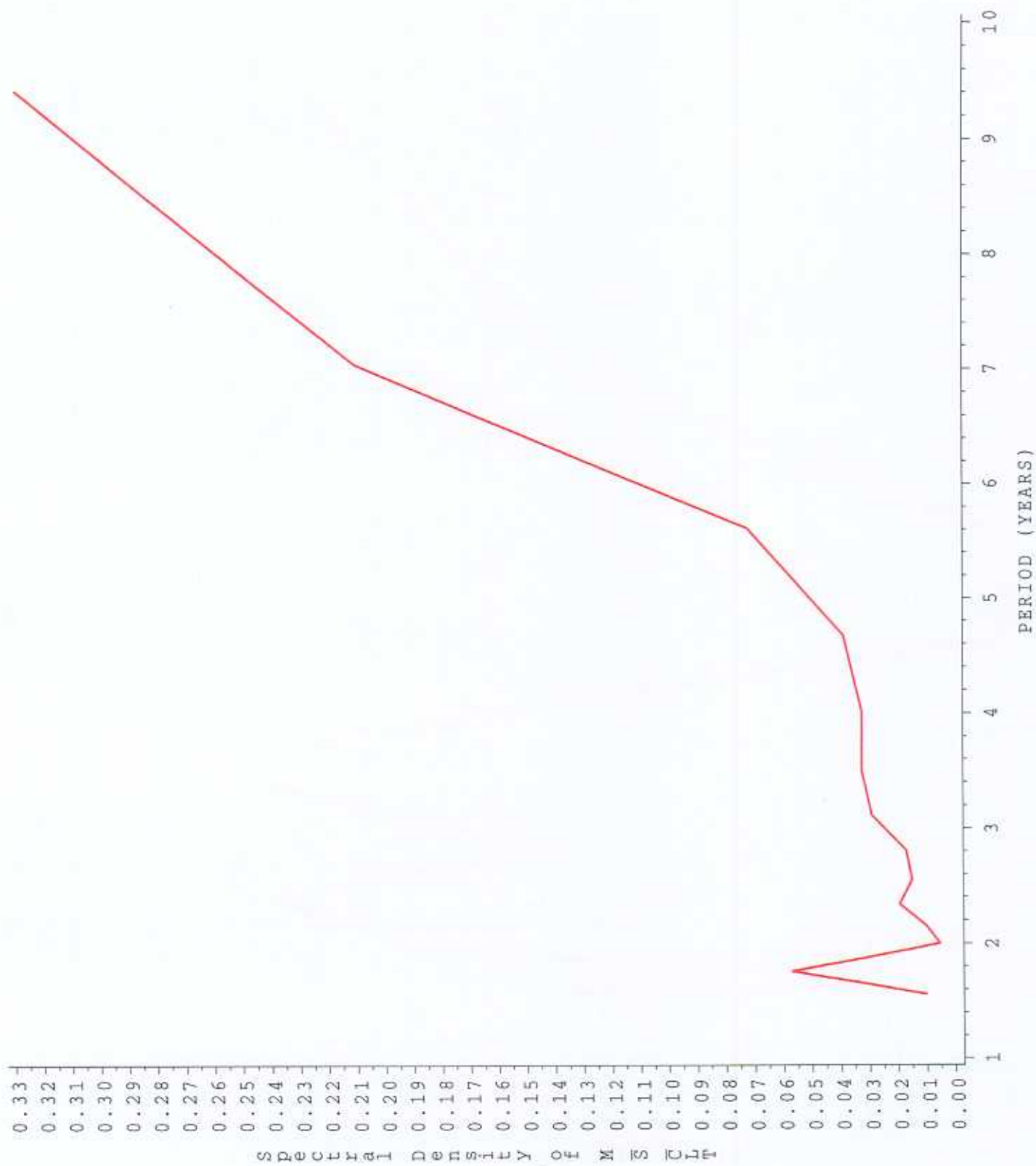


Fig. 38. Spectral density of wind speed for CLT

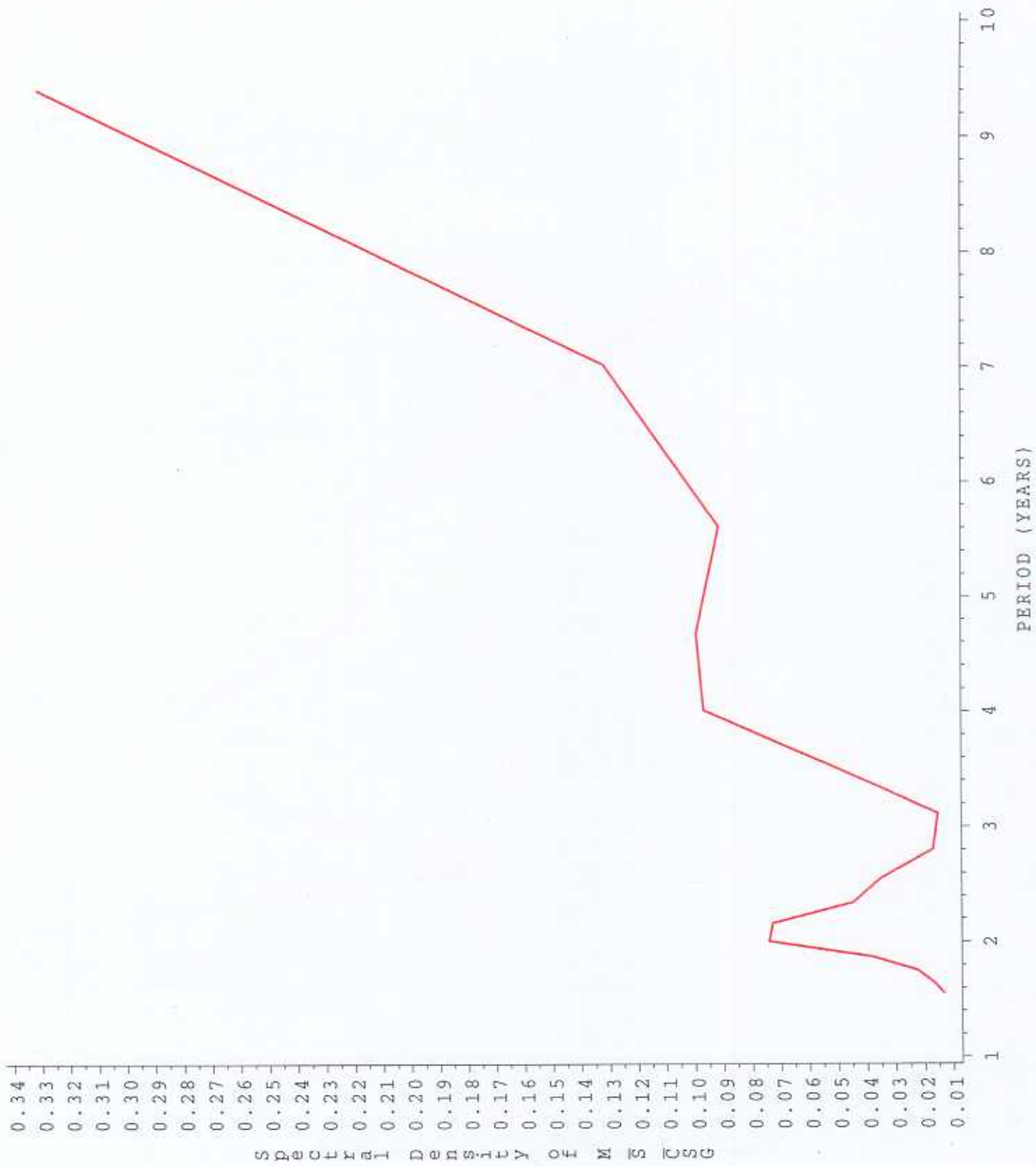


Fig. 39. Spectral density of wind speed for CSG₅₅

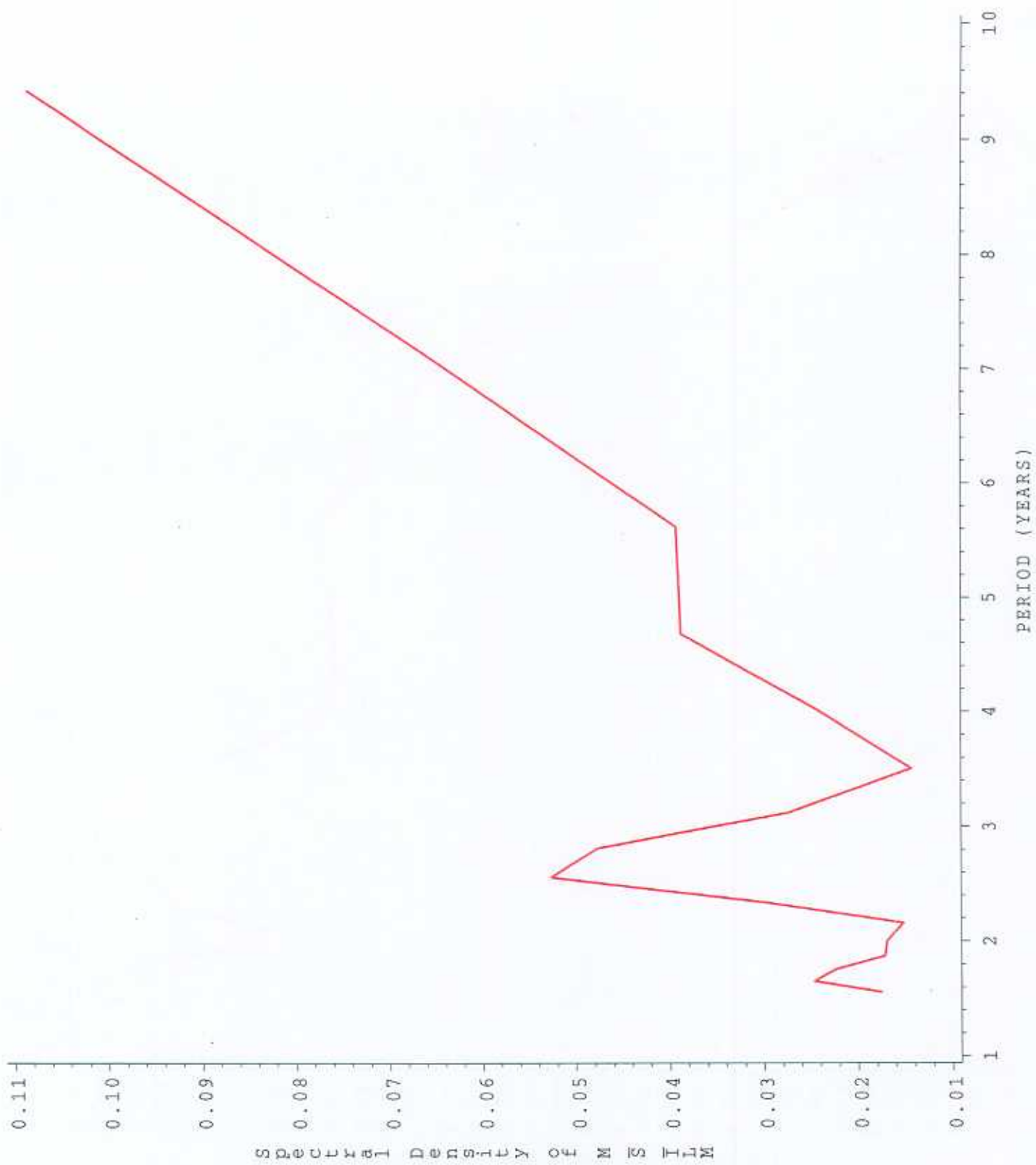


Fig. 40. Spectral density of wind speed for ILM

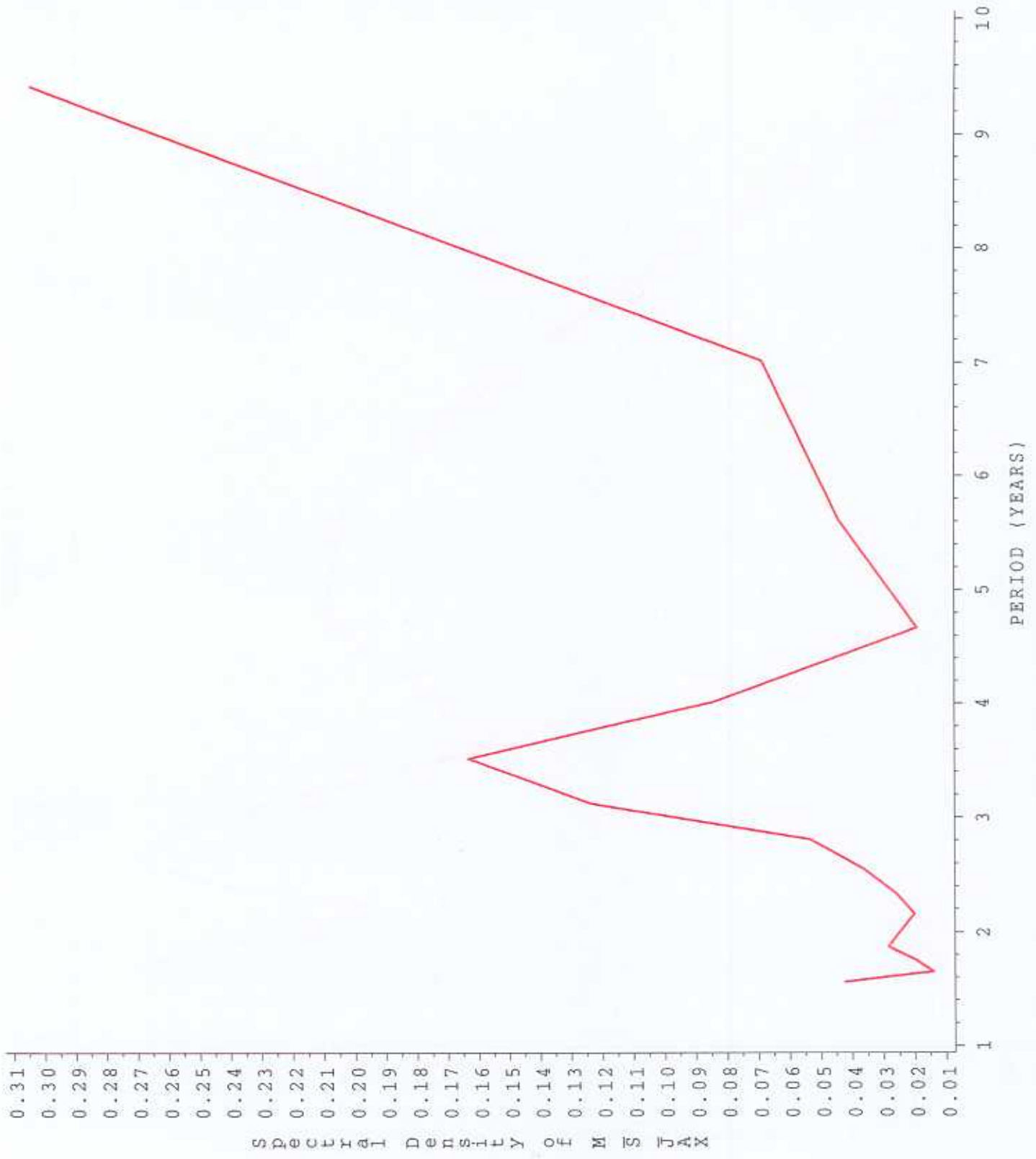


Fig. 41. Spectral density of wind speed for JAX

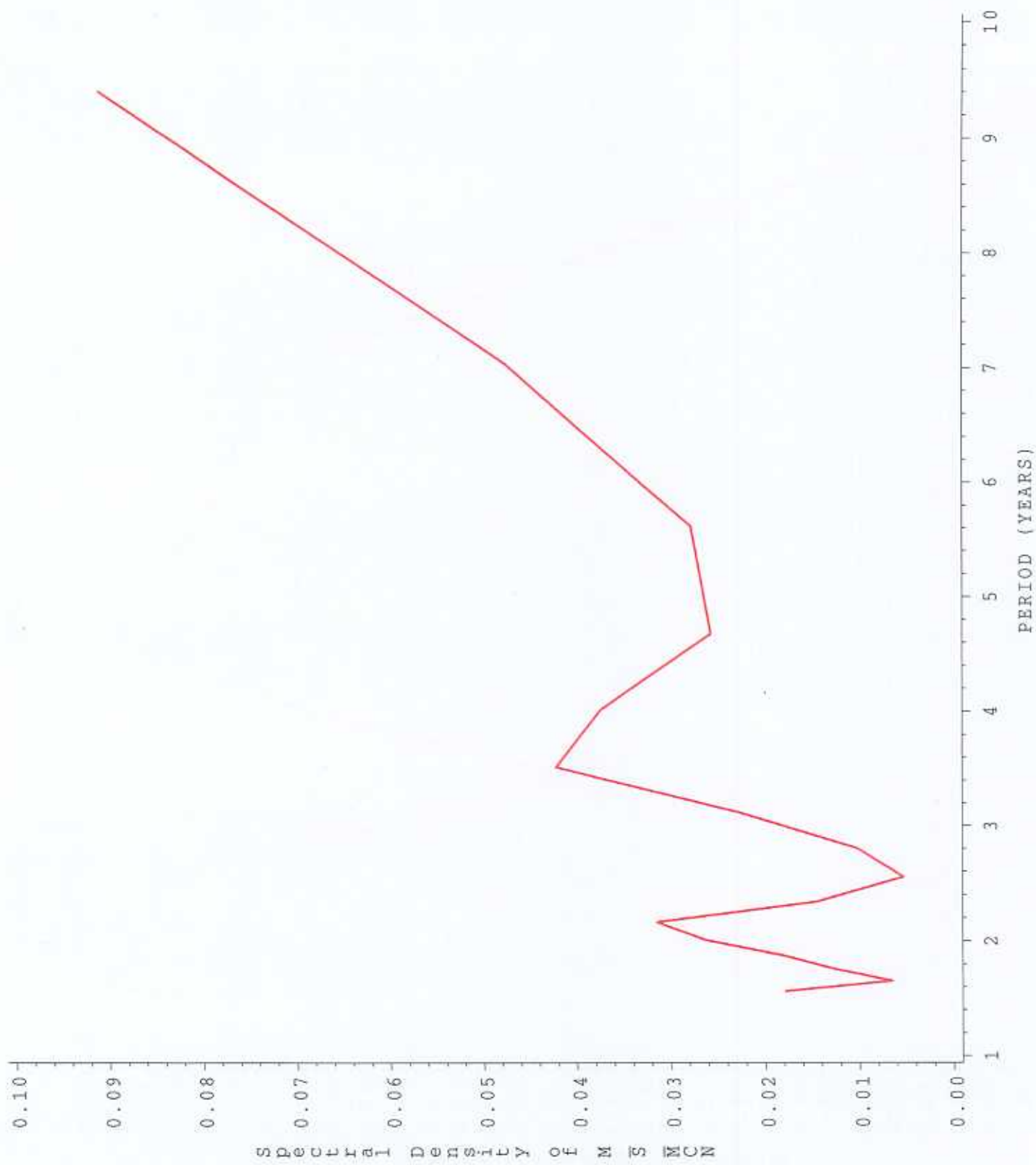


Fig. 42. Spectral density of wind speed for MCN

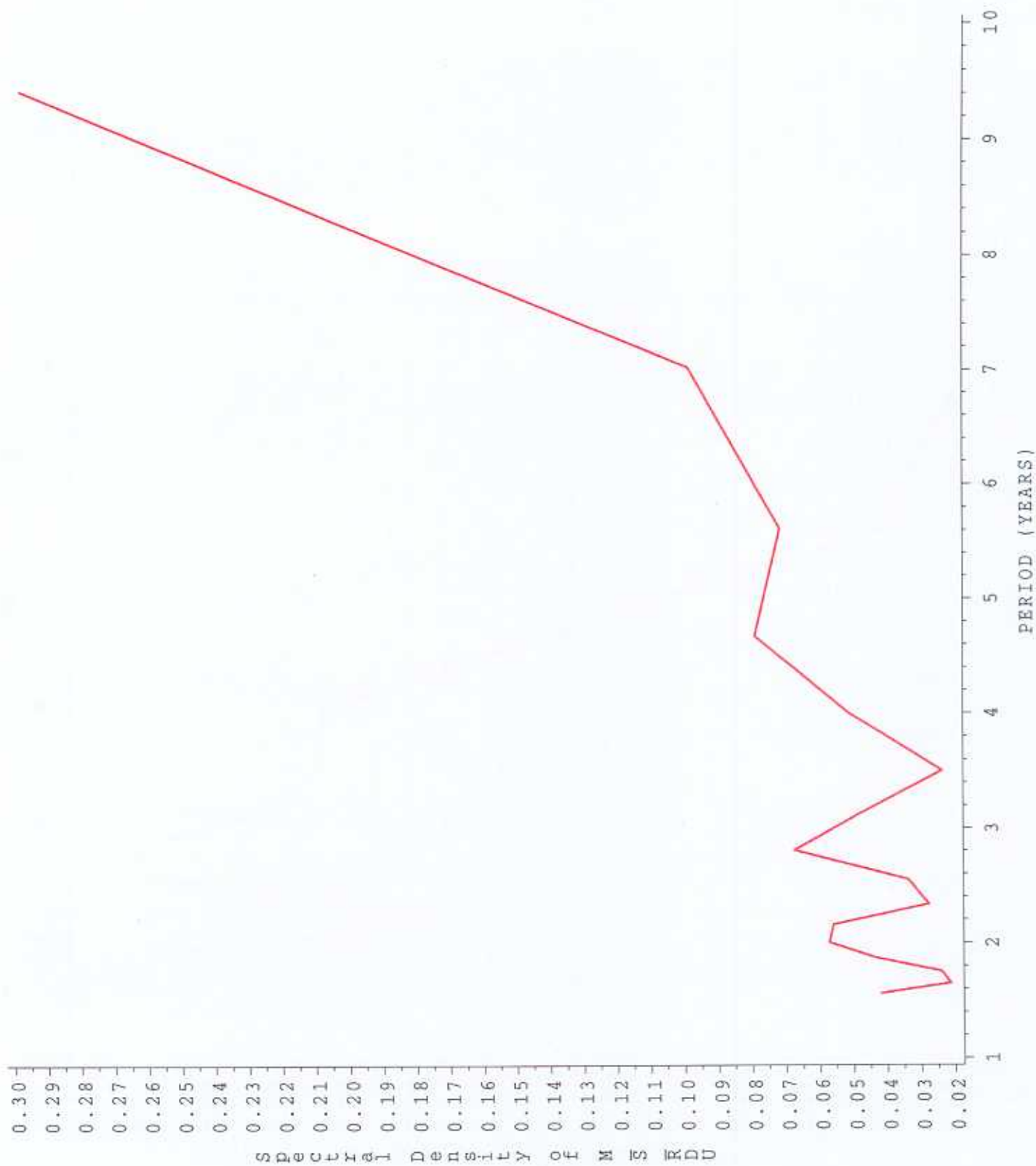


Fig. 43. Spectral density of wind speed for RDU₅₉

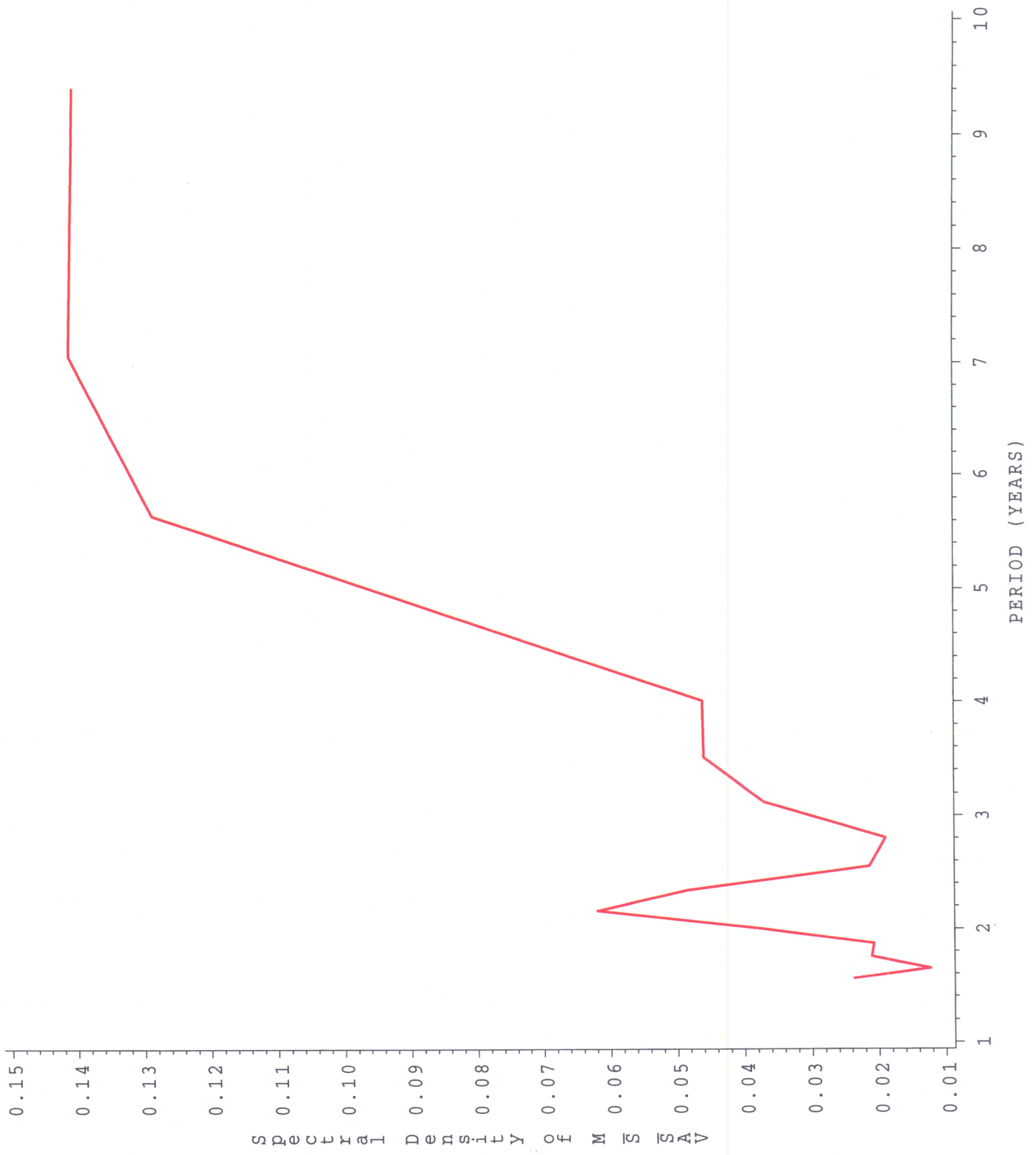


Fig. 44. Spectral density of wind speed for SAV